POLYPUBLIE
Polytechnique Montréal

POLYTECHNIQUE MONTRÉAL
UNIVERSITÉ D'INGÉNIERIE

Titre: Title:	Hysteresis modeling in EMTP-RV
Auteur: Author:	Sébastien Dennetière
Date:	2003
Type:	Mémoire ou thèse / Dissertation or Thesis
Référence: Citation:	Dennetière, S. (2003). Hysteresis modeling in EMTP-RV [Mémoire de maîtrise, École Polytechnique de Montréal]. PolyPublie. https://publications.polymtl.ca/7044/

Document en libre accès dans PolyPublie
Open Access document in PolyPublie

URL de PolyPublie: PolyPublie URL:	https://publications.polymtl.ca/7044/
Directeurs de recherche: Advisors:	Xuan-Dai Do, & Jean Mahseredjian
Programme: Program:	Non spécifié

UNIVERSITÉ DE MONTRÉAL

HYSTERESIS MODELING IN EMTP-RV

SÉBASTIEN DENNETIÈRE

DÉPARTEMENT DE GÉNIE ÉLECTRIQUE ET

DE GÉNIE INFORMATIQUE

ÉCOLE POLYTECHNIQUE DE MONTRÉAL

MÉMOIRE PRÉSENTÉ EN VUE DE L'OBTENTION

DU DIPLÔME DE MAÎTRISE ÈS SCIENCES APPLIQUÉES

(GÉNIE ÉLECTRIQUE)

MAI 2003

Canada

UNIVERSITÉ DE MONTRÉAL

ÉCOLE POLYTECHNIQUE DE MONTRÉAL

Mémoire intitulé :

HYSTERESIS MODELING IN EMTP-RV

présenté par : DENNETIÈRE Sébastien

en vue de l'obtention du diplôme de : Maîtrise ès sciences appliquées

a été dûment accepté par le jury d'examen constitué de :

M. OLIVIER Guy, Ph.D., président

M. DO Xuan-Dai, Ph.D., directeur de recherche

M. MAHSEREDJIAN Jean, Ph.D., co-directeur de recherche

M. JOOS Geza, Ph.D., membre

Acknowledgements

I would like to express my appreciation to all the people who contributed, directly or indirectly, to the realization of this research project.

On a sad note, Dr Xuan-Dai Do passed away during the realization of this work. He will be always remembered.

I would like to thank Dr Jean Mahseredjian for making me understand that science is above all a human activity. Even if he spent incalculable hours to carry on the EMTP-RV project with a impressive faith, he gave to me a lot of time to realize this project. I am very proud to have been directed by such a person.

When I started my research project at IREQ, Benoît Delourme who worked for EDF (Électricité de France) showed me that programming is less frightening than it appears. He was very patient in explaining to me various concepts and showed me to be patient when looking at existing large program codes.

Omar Saad was also always helpful when problems occurred in the hysteretic reactor code. He helped me to find simple solutions to complex problems. My workmate, Niko Qako, always gave me answers in asking me questions.

This research project has been done as part of a student exchange agreement between Supélec (École Supérieure d'Électricité) and École Polytechnique de Montréal. Patrick Bastard was the professor in charge at Supélec for my studies in Canada. He is the person who made me appreciate power systems. Dr Gilles Roy at École Polytechnique de Montréal spent a lot of time to solve my administrative problems and strived to find better courses during my study.

I realized this work in a nice working atmosphere, I met a lot of nice people such as Pierre-Olivier Dallaire and Marie Viutti.

Living in a foreign country is not always easy and I would like to simply say thanks to Catherine for her listening and understanding: Youkali is not far.

To finish these acknowledgements I would like to express my huge gratitude to the two most important people in my life: my parents.

Summary

The contribution of the present work consists of a new mathematical representation of the hysteresis phenomenon. The model is constructive in that all functions can be determined from a given measurement. It is sufficiently simple and is, therefore, applicable for numerical simulations.

The new hysteretic reactor has been implemented in the new EMTP code, named EMTP-RV [1][2]. The challenge of an EMTP type model is to correctly simulate hysteresis with the inherent complexities related to minor loops. The most commonly used hysteretic reactor model in EMTP (previous version) is the pseudononlinear Type-96 model [3]. The pseudononlinear term implicates that the reactor is not solved simultaneously with the surrounding network equations. In addition to the well known limitations of such an approach, the Type-96 modeling assumptions make it a poorer candidate for matching experimental results.

In addition to the Type-96 model, EMTP has recently introduced the Type-92 model [3]. It remained however prone to numerical problems and limitations mainly due to the applied solution method for true-nonlinear models. Other aspects, such as the data fitting procedure, were using a less accurate method.

This work starts by a summarized presentation on common hysteresis models and on the limitations of the previously available EMTP models. It follows by the presentation of a new solution method for a physical model derived from [4] and [5]. Other details on the actual model are also provided. The new implementation demonstrates unsurpassed capability for the simulation of large scale networks with hysteretic reactors located in arbitrary network configurations. A practical test case taken from the EDF (Électricité de France) power system [17] is shown to attain good numerical accuracy without degrading simulation performance.

Abstract

This work presents the implementation of a hysteretic reactor model in a transient analysis package. The model is available in a currently developed EMTP (DCG-EPRI) version. EMTP is the Electromagnetic Transients Program. A computer application widely used for the simulation and analysis of transients in power systems.

It is demonstrated how the hysteretic reactor equations can be solved to eliminate topological limitations and allow solving large scale networks efficiently. Numerical robustness aspects and the representation of minor loops are emphasized. The model demonstrates new and not previously available computational capabilities.

A series of simulation tests were performed on practical networks in order to assess the validity of the model. The results from these tests indicate that the model is accurate, fast, and reliable.

Condensé en français

1 Introduction

Le phénomène d'hystérésis magnétique joue un rôle très important dans l'analyse de certains cas de systèmes de puissance. Les exemples pratiques les plus connus sont les courants d'envahissement (inrush currents) et la ferroresonance. De plus l'inclusion d'une branche hystérétique dans le modèle d'un transformateur permet la représentation des flux résiduels et fournie une modélisation plus précise des pertes.

Ce mémoire présente le travail réalisé dans le cadre de ma maîtrise recherche. Il avait pour but final l'implémentation d'un modèle de réactance hystérétique dans un logiciel de simulation de phénomènes électromagnétiques transitoires. Le modèle est disponible dans la version la plus récente du logiciel EMTP (Electromagnetic Transients Program).

Après avoir débuté par une recherche bibliographique concernant les différentes modélisations du phénomène d'hystérésis, je me suis intéressé plus particulièrement aux modèles implémentés dans les anciennes versions d'EMTP. Ces modèles avaient l'avantage d'avoir un historique de validation important. C'est pourquoi la base du modèle présenté dans ce mémoire est inspirée d'un modèle d'hystérésis disponible sous EMTP-V3. Ce modèle, dit de Type 92, a été validé par des mesures expérimentales réalisées par Ontario Hydro à Cherrywood TS sur des transformateurs de puissance [4].

Les équations du modèle ont ensuite été converties afin d'être adaptées à l'environnement numérique d'EMTP-RV. Des problèmes de résolution numériques tels que l'initialisation en régime permanent ont été résolus. Il a aussi été nécessaire d'inventer une formulation numérique pour résoudre les équations non linéaires par une méthode de Newton-Raphson. Cette contrainte est essentielle pour solutionner de façon simultanée des réseaux de grande envergure incluant de nombreuses non linéarités. Ces formulations numériques ont ensuite été suivies d'une série de tests de validation. Un programme indépendant d'EMTP-RV, et calculant les paramètres du modèle avant la simulation, a aussi fait l'objet d'un codage complet en FORTRAN 95.

Pour introduire ce mémoire un état de l'art dans le domaine de la modélisation du phénomène d'hystérésis est préalablement réalisé. Les modèles déjà implémentés dans les anciennes versions d'EMTP sont étudiés dans ce cadre. Les raisons pour lesquelles les anciens modèles ont été abandonnés sont aussi expliquées.

La théorie du modèle nouvellement implémentée, basée sur celle d'un modèle existant, est ensuite analysée. Il est ensuite démontré comment la nouvelle implémentation élimine les restrictions topologiques et permet ainsi la résolution de réseaux de grande échelle de façon efficace.

De nombreux tests montrent une robustesse et une efficacité, jusqu'alors non disponibles, dans la modélisation du phénomène d'hystérésis.

2 Les modèles disponibles dans EMTP-V3

Les modélisations du phénomène d'hystérésis peuvent être classées en 3 grands groupes. Le premier, basé sur les propriétés magnétiques des matériaux, nécessite la résolution d'équations différentielles. Ce type de modèle nécessite beaucoup de données et la résolution numérique des équations se révèle être très complexe. Le deuxième groupe de modélisations se base sur la théorie de Preisach qui utilise essentiellement des procédures d'interpolation. La complexité de ces modèles les rend difficilement implémentables dans des programmes de simulation numérique.

Les modèles appartenant au troisième groupe sont basés sur des considérations géométriques. Les équations prennent en compte les formes expérimentales des courbes d'hystérésis. Les modèles implémentés dans EMTP-V3 appartiennent à cette catégorie de modélisation.

2.1 Le modèle communément utilisé dans EMTP-V3 : la réactance hystérétique Type-96

2.1.1 Théorie du modèle

Les cycles d'hystérésis sont ici modélisés par des segments de droite. Des interpolations linéaires sont réalisées entre chaque points de la caractéristique donnée par l'utilisateur. C'est pourquoi ce modèle est dénommé « pseudo non-linéaire ».

Les données nécessaires au modèle se réduisent à la branche croissante du cycle principal d'hystérésis donnée sous forme de coordonnées dans le plan Flux/Courant (voir la figure qui suit). Il est admis qu'au delà des valeurs extrêmes de flux et de courant, le cycle d'hystérésis n'a plus d'épaisseur.

La prise en considération de l'existence de cycles mineurs est ici très simple. Les sous-cycles sont en fait déduits du cycle principal par homothétie. Cette transformation est conditionnée par la nécessité de fermeture des sous-cycles.
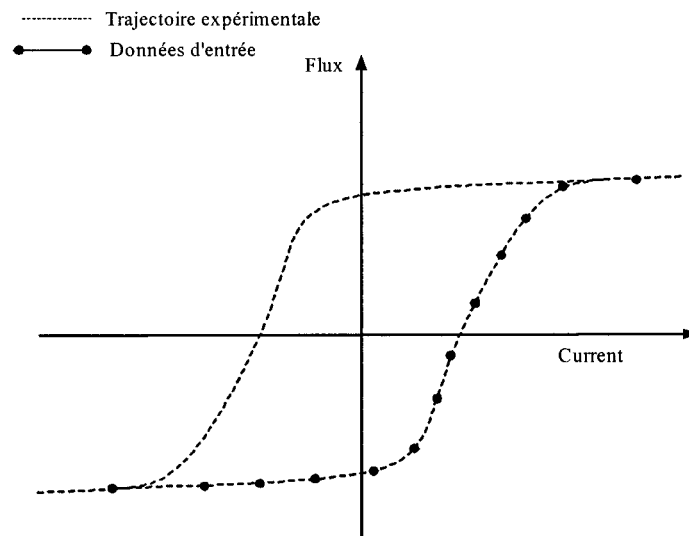
Figure 2-1 Caractéristique nécessaire au modèle du Type-96 dans EMTP-V3

2.1.2 Problèmes théoriques du modèle TYPE96

Ce modèle conceptuellement simple semble être mis souvent en défaut par des tests expérimentaux. En effet l'existence d'une épaisseur de cycle nulle à partir d'un certain niveau de saturation n'est basée sur aucune validation physique. D'autre part la forme des trajectoires hystérétiques des sous-cycles semble plus complexe qu'une simple translation du cycle majeur. Ensuite les cycles mineurs peuvent parfois rester ouverts à cause du manque d'information stockée sur leur parcours.

La réactance Type-96 est un élément non-linéaire pour lequel la résolution avec le réseau n'est pas simultanée. Le programme va changer le segment d'opération uniquement après avoir réalisé que le point courant était en dehors d'une région légale. Ce problème se traduit par des trajectoires peu précises (Figure 2-2).
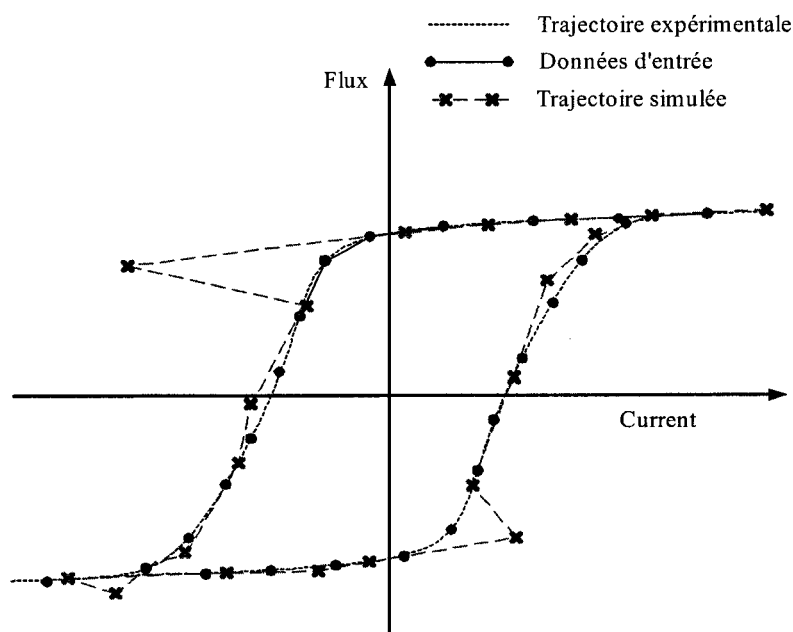
Figure 2-2 Modèle Type-96 : Changement de segment après une opération illégale

2.2 Un modèle purement non-linéaire : la réactance de Type-92

EMTP (la version V3) a ajouté récemment le modèle d'hystérésis de Type-92. Ce modèle défini comme étant purement non-linéaire est apte à être résolu simultanément avec le réseau. Par contre le modèle possède plusieurs problèmes numériques. Il n'est pas simple à généraliser et impose des contraintes topologiques aux réseaux simulés. La formulation de l'ensemble du modèle est donc à revoir.

3 Le modèle implanté

3.1 Principes de base du modèle

Le principe de base de la modélisation présentée dans ce mémoire est la décomposition des trajectoires d'hystérésis en deux mouvements indépendants : l'un dû à la saturation et l'autre dû à l'hystérésis pure. Des résultats expérimentaux approuvent cette hypothèse et plusieurs observations donnent les autres bases du modèle :

- La forme des courbes de magnétisation suivant un point d'inversion semble suivre un modèle simple pouvant être translaté de sous-cycles en sous-cycles. Ce canevas de base aurait pour point d'origine les points d'inversion.

- Chaque courbe revient toujours à l'avant dernier point d'inversion pour fermer les sous-cycles.

- Immédiatement après avoir dépassé un point d'inversion, le canevas de base est décalé afin de refermer le sous-cycle en cours.

3.1.1 Les équations du modèle

La réactance hystérétique est modélisée par une fonction non-linéaire qui relie le flux instantané au courant en deux étapes. Deux différentes fonctions sont ainsi définies :

- Une fonction d'hystérésis pure reliant le flux « non saturé » λ_{unsat} au courant.

- Une fonction de saturation pure reliant le flux instantané λ_{sat}, nommé flux « saturé », au flux « non saturé » λ_{unsat}.

Les fonctions d'hystérésis et de saturation sont basées sur des équations quadratiques.

D'abord le flux instantané est relié au flux « saturé » par une équation dite de saturation (3.1).

$$C_{sat} = \left[\lambda_{unsat} - \frac{\lambda_{sat}}{S_{sv}} - X_{sv} \right] \left[S_{sh}.\lambda_{unsat} - \lambda_{sat} + Y_{sh} \right] \qquad (3.1)$$

La constante C_{sat} définit la courbure, elle contrôle le rapprochement de la courbe avec ses asymptotes. S_{sv} est la pente de l'asymptote verticale, S_{sh} est la pente de l'asymptote horizontale, X_{sv} est l'abscisse à l'origine de l'asymptote verticale et Y_{sh} est l'ordonnée à l'origine de l'asymptote horizontale. Une fois la forme de la courbe de saturation définie, la partie concave de la fonction est prise pour les valeurs positives de λ_{unsat} et λ_{sat}. La relation entre les valeurs négatives est obtenue par symétrie. La courbe finale de saturation passe par l'origine.

La relation reliant λ_{unsat} et i est donnée par

$$C_{hyst} = \left[i - \frac{\lambda_{unsat}}{S_{hv}} - X_{hv} \right] \left[S_{hh} i - \lambda_{unsat} - Y_{hh} \right]$$

$$(3.2)$$

La constante C_{hyst} définit l'effet de courbure de l'hystérésis. Les autres variables sont définies comme dans l'équation (3.1), mais pour le phénomène d'hystérésis. Dans ce cas la branche convexe est choisie pour les trajectoires croissantes et la branche concave pour les trajectoires décroissantes. Puisqu'il faut définir un cycle fermé, un mouvement de translation est réalisé sur les asymptotes. La Figure 3-1 montre la courbe initiale (ligne continue bleue) et la courbe translatée (ligne pointillée rouge). Les courbes de trajectoires croissante et décroissante forment le cycle complet.
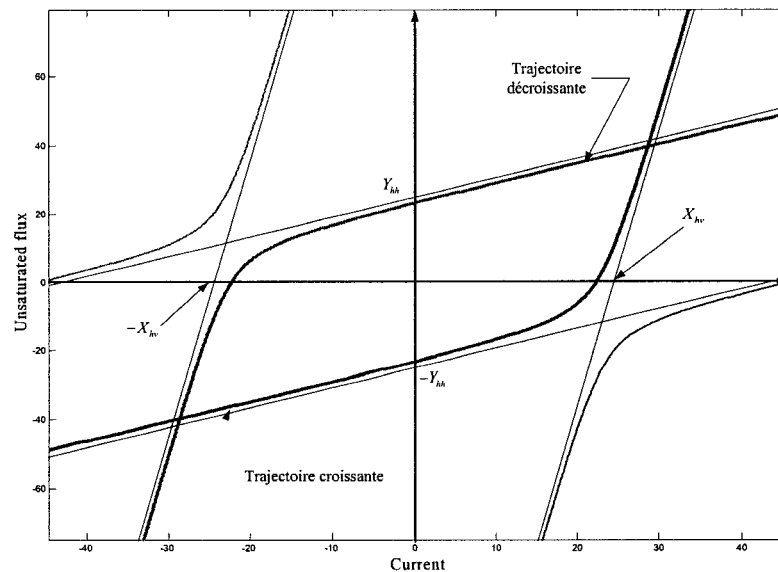
Figure 3-1 Canevas de base du modèle d'hystérésis

3.1.2 Les trajectoires d'hystérésis

Les trajectoires hystérétiques suivent un modèle de canevas. Les trajectoires croissantes et décroissantes correspondent à des orientations opposées du canevas. Les paramètres X_{hv} et Y_{hh} contrôlent la position du canevas et sont systématiquement modifiés lors de la simulation. Les paramètres C_{hyst}, S_{hv} et S_{hh} sont fixes et définissent la forme du canevas. Puisque la forme du canevas est indépendante de sa position, le point de départ d'une trajectoire (point d'inversion sur le cycle d'hystérésis) est choisi comme origine du système de coordonnées. Ainsi, en accord avec le modèle, l'asymptote verticale (de pente S_{hv}) est déplacée à droite (ou à gauche pour une trajectoire décroissante) le long de l'axe des abscisses d'une distance égale à deux fois le courant coercitif. La trajectoire d'un cycle mineur ne peut dépasser les asymptotes verticales du cycle principal.

Lorsqu'un point d'inversion est détecté une nouvelle trajectoire commence. Un point d'inversion apparaît lorsque le flux $\Phi(t + \Delta t) < \Phi(t)$ sur une trajectoire croissante

ou lorsque $\Phi(t + \Delta t) > \Phi(t)$ sur une trajectoire décroissante. Le point d'inversion créant ainsi le sous-cycle doit être sauvé. Les branches hyperboliques passent automatiquement par l'avant dernier point d'inversion. La Figure 3-2 illustre la progression de la trajectoire à partir d'un cycle interne A. Lorsque le flux augmente au delà du point 5, le point d'inversion qui définit la trajectoire est le point 4. C'est pourquoi une pile de points d'inversion composée des valeurs (λ_{unsat}, i) est utilisée pour sauver les points en dehors du cycle en cours de parcours.
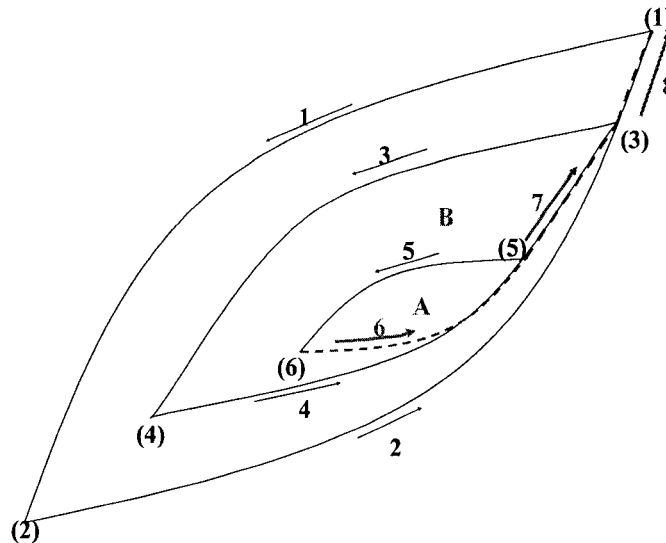
Figure 3-2 Points d'inversion dans les trajectoires hystérétiques

4 Implémentation dans EMTP

4.1 Le programme de calcul des paramètres

Dans un premier temps il est nécessaire de déterminer les paramètres du modèle à partir des données expérimentales. Le nouveau programme utilisé pour réaliser cette tâche a recours à une méthode de moindres carrés pour trouver les paramètres de saturation de l'équation (3.1). Le paramètre S_{hv} de l'équation (3.2) est aussi déterminé par cette méthode puisque durant le processus de calcul λ_{unsat} est remplacé par $S_{hv} i$. Le reste des paramètres de l'équation (3.2) sont déterminés à partir des données des cycles mineurs. Le courant coercitif est déterminé à partir des données du cycle majeur, ou peut être donné manuellement. On permet ensuite à l'utilisateur de visualiser les résultats et ainsi de les modifier à sa convenance.
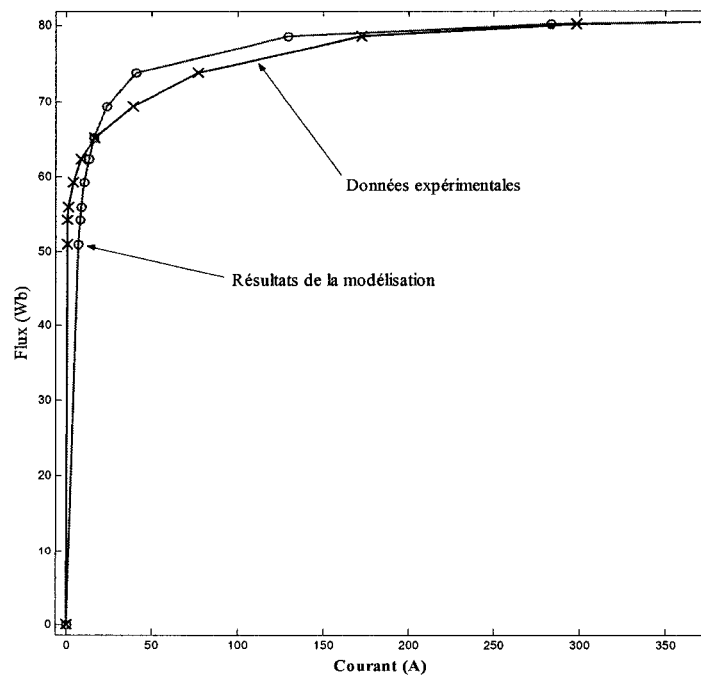

Figure 4-1 Résultats de la détermination des paramètres du modèle

La Figure 4-1 compare des données expérimentales et le résultat de la modélisation. La symétrie imposée par les branches hyperboliques complique le processus de détermination des paramètres si les données d'entrée manquent de symétrie.

Il est aussi à noter que le phénomène d'hystérésis peut dépendre de paramètres qui ne sont pas des donnés d'entrée du modèle. Par exemple pour le cas d'une possible dépendance en température du phénomène, l'utilisateur peut la prendre en considération s'il possède les courbes de saturation pour différentes températures.

4.2 Circuit équivalent

La nouvelle réactance hystérétique a été implémentée dans le nouveau code d'EMTP, nommé EMTP-RV. Afin d'obtenir une solution complètement générale pour laquelle les modèles non-linéaires peuvent être résolus sans restriction topologique, EMTP-RV utilise une résolution itérative avec le système des équations linéaires en entier. Les éléments non-linéaires doivent simplement retourner leur circuit de Norton équivalent discrétisé correspondant au point d'opération en cours. Ceci constitue une méthode de Newton-Raphson.

Dans EMTP-RV, la réactance hystérétique est un élément dont la donnée d'entrée est le flux et la donnée de sortie le courant. A chaque pas de temps elle est transformée en son équivalent de Norton présenté à la Figure 4-2. C'est cette technique qui est utilisée pour l'inductance non-linéaire. Le flux $\Phi_t^{(j)}$ (au temps t lors de l'itération j) est d'abord trouvé à partir des tensions en utilisant la méthode d'intégration trapézoïdale avec un pas de temps Δt :

$$\Phi_t^{(j)} = \frac{\Delta t}{2} v_t^{(j)} + \Phi_{history_t} \tag{4.1}$$

Ce flux est ensuite rentré dans l'équation (3.1) comme étant λ_{sat} pour trouver λ_{unsat} et ensuite dans l'équation (3.2) pour trouver le courant sur la trajectoire ainsi que $\Phi_{q_t}^{(j)}$ (ordonnée à l'origine du segment d'opération) dans :

$$\Phi_t^{(j)} = K_{q_t}^{(j)} \, i_t + \Phi_{q_t}^{(j)}$$

(4.2)

Le calcul de $K_{q_t}^{(j)}$ nécessite la différentiation des équations (4.3) et (4.4). Il est enfin montré que la combinaison de (4.1) et de (4.2) donne :

$$i_t = \frac{\Delta t}{2 K_{q_t}^{(j)}} \, v_t + \frac{1}{K_{q_t}^{(j)}} \left(\Phi_{history_t} - \Phi_{q_t}^{(j)} \right)$$

(4.5)

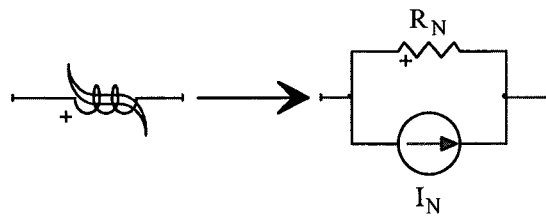qui correspond au circuit de la Figure 4-2.

Figure 4-2 Circuit équivalent de la réactance hystérétique

5 Conclusions

Ce mémoire présente l'implémentation d'une nouvelle réactance hystérétique dans un logiciel de simulation de phénomènes transitoires. Le modèle a été décrit en utilisant l'environnement EMTP-RV. Le modèle en tant que tel provient d'un modèle déjà existant mais sa résolution numérique ainsi que son implémentation sont nouvelles.

La résolution de problèmes importants tels que l'initialisation, la détermination des paramètres, et l'intégration dans une méthode de Newton-Raphson a été réalisée. Les principaux avantages de cette nouvelle implémentation en comparaison avec les précédentes formulations peuvent être résumés comme suit :

- Ce modèle purement non-linéaire a l'aptitude d'être résolu simultanément avec le réseau et cela avec des configurations topologiques quelconques. EMTP-RV, utilise une méthode itérative avec l'ensemble des éléments linéaires afin de procéder à une résolution de Newton-Raphson complète. Cette méthode augmente de façon substantielle la probabilité de convergence du modèle pour un pas de temps donné.
- La méthode de détermination des paramètres du modèle a été grandement améliorée pour diminuer la différence entre les données d'entrée et les résultats de la simulation.
- Le modèle est précis et son utilisation dans un réseau de puissance n'augmente pas de façon significative le temps de calcul en comparaison avec l'utilisation du modèle d'inductance non-linéaire.

Le modèle a été testé, avec succès, dans de nombreux cas d'énergisation de transformateurs.

Le présent travail de recherche peut être poursuivi dans deux directions. D'abord il serait possible d'utiliser des équations d'ordre 3 ou 4 au lieu d'équations quadratiques. Ce changement permettrait de diminuer la contrainte de symétrie des données d'entrée

pour obtenir une modélisation plus précise. Une autre piste de recherche serait la prise en compte de la dépendance en fréquence du phénomène d'hystérésis.

L'implémentation dans la version officielle d'EMTP-RV donne à ce modèle une application d'envergure industrielle. Les structures de programmation « orientées objet » présentent une modularité et une flexibilité complètes. Le travail présenté dans ce mémoire pourra être ainsi facilement enrichi et il donnera la possibilité d'étendre la recherche dans ce domaine.

Table of contents

List of Figures

1 Introduction

The ferromagnetic core transformer is an element commonly encountered in power systems circuits. It is essential to represent this component accurately in simulation studies and, in particular, to include its nonlinear properties. Magnetic saturation and hysteresis are among the important nonlinear phenomena associated with the transformer core.

Magnetic hysteresis plays an important role in power system problems, such as the inrush current and ferroresonance. It is responsible for the residual flux and, for the damping of electromagnetic transients. To analyze electric power circuits containing ferromagnetic elements, it is necessary to develop a technique for simulating the hysteresis phenomenon.

Basically two different approaches have been used in the past to solve this modeling problem. One approach is based on the physical principles governing the device, and usually takes the form of partial differential equations. In theory, this approach is the most appealing because if carried out properly, the model could be quite realistic. Unfortunately, the physical principles governing most hysteretic elements are not well understood in general. Even in the case where there is a reasonably good physical understanding, as in the case of an inductor exhibiting hysteresis, one is usually forced to make various idealizations in order to translate the physical principles into appropriate partial differential equations. In so doing, one could only hope that the simplifying assumptions will not alter significantly the accuracy of the model.

The second approach is based on postulating suitable mathematical implementation, which can be shown to exhibit hysteresis phenomenon. Since practically all elements or systems exhibiting hysteresis are nonlinear, these mathematical representations must necessarily be nonlinear. Unfortunately, in the absence of a practical representation theorem analogous to that for linear systems it would require an infinite set of complete measurements corresponding to all excitation signals in order to establish the validity of a nonlinear model. Hence, the main difficulty inherent to in the second modeling approach

is that the validity of the model can only be established qualitatively. This consists of first showing that the postulated mathematical representation exhibits the same significant properties and features of the hysteretic element. Then appropriate functions and parameters of the mathematical model are constructed so that the resulting model would yield realistic response.

This document presents the implementation of a new hysteretic reactor model in a software named EMTP-RV. EMTP-RV [1] is the latest "new generation" version of EMTP [3]. EMTP, the Electromagnetic Transients Program, is an advanced software for the simulation of transients in power systems. Arbitrary network topologies can be assembled through a graphical user interface (name EMTPWorks [2]), simulated and analyzed. EMTP is applied for simulations from lightning to steady-state operating conditions. EMTP has two main computation modules: the steady-state module and the time-domain. The steady-state module is an option for automatic computation of initial operating conditions. The time-domain module is for automatic computations of detailed waveforms for various system variables.

Although EMTP and EMTP-RV are based on similar paths and are historically related, EMTP-RV offers a completely different computation system. Both the linear system equations and the nonlinear solver are significantly different.

The contribution of this work is the complete "programming" of a new hysteretic reactor model in EMTP-RV. The project starts from an existing behavioral model of the hysteresis effect in power transformers. The selected behavioral model validity, as such, has been confirmed in the literature and in laboratory reports [4]. The "programming" contribution includes several steps. The model equations are first converted to become suitable for the numerical environment available in EMTP-RV. Specific automatic computation problems, such as initialization, have been solved. It was then needed to invent a formulation for solving the nonlinear model equations through a Newton method within the performance criterion of very high rate convergence. Such criterion is essential for solving large scale systems with multiple nonlinearities. The derived numerical

formulations are followed by actual implementation and testing. Other aspects, such as fitting of measured data to model equations, are also contributed.

The presentation in the following sections starts from a background survey on existing nonlinear core models. It is then followed by the presentation and discussion of numerical models that were available in previous EMTP versions. The reasons for abandoning those models are explained by focusing on numerical weakness, lack of generalization and practical validity. The selected model behavioral equations are then presented before entering into the details of the actual numerical solution, also referred to as "implementation". Test cases are used to demonstrate the new EMTP-RV model.

2 Background on existing nonlinear core models

A variety of models for representing magnetic hysteresis have been presented in the literature and these models can be classified into three groups. The first group comprises models that are based on physical properties of the magnetic materials such as domain wall movement. The Jiles-Atherton model [6], for example, derives first order nonlinear differential equations. However, the model is quite complex and it depends on several empirical quantities which are obtained by fitting experimental data. The second category consists of models based on Preisach's theory [7] and these are essentially curve fitting procedures. Unfortunately, these models are complex and may not be easily incorporated into simulation programs. Models belonging to the third category are based on geometrical considerations. Equations take into account experimental shapes of hysteretic curves. The hysteretic theory presented in this work is based on a model that belongs to the third category.

2.1 Models based on Jiles-Atherton theory

2.1.1 Solution of the differential equation

The mathematical model for ferromagnetic hysteresis introduced by Jiles and Atherton in 1983 [6] is based on physical principles, rather than strictly mathematical arguments or experimental curve fitting.

In this theory the magnetization in a ferromagnetic material is given by M, the magnetic field intensity by H, the magnetic flux density by $B = m_0(H + M)$, and the effective flux density (of the Weiss mean field) by $B_e = \mu_0(H + \alpha M)$. The differential equation for M is then:

$$M = M_s \, L\left(\frac{B_e}{a}\right) - k\delta\left(\frac{dM}{dBe}\right)$$

(2.1)

where:

$$L(x) = \coth(x) - \frac{1}{x} \tag{2.2}$$

L(x) is the Langevin function, M_s, a, and k are parameters of the model, and δ is the

sign of $\dfrac{dH}{dt}$.

If the parameters a and k are constants or functions of B_e only, then (2.1) is a first order, linear differential equation whose solutions may be obtained by standard methods. The solution to the corresponding homogeneous equation is:

$$M_h = M_0 \exp\left(-\delta \int_0^{B_e} \frac{1}{k} dB_e\right) \tag{2.3}$$

where M_0 is a constant. Then the complete solution is $M = M_h + M_p$ where:

$$M_p = M_h \delta \int \frac{M_s L(B_e/a)}{kM_h} dB_e \tag{2.4}$$

If the parameters a and k are not constants, then the solution for (2.1) can be obtained as a series by iteration in the differential equation as an alternative to solving the integrals in (2.3) and (2.4).

2.1.2 Implementation of the model

The minor loops are not obtained from a differential equation, but require evaluation of transcendental functions of the fields at the extremes of the minor loops in order to be able to calculate magnetizations along the loops. This method does not lend itself to the calculation of magnetizations for arbitrary transient excitations where the turning points are not known a priori.

The Jiles-Atherton hysteresis models presented two majors advantages: only five model parameters and parameter determination is possible by using only one measured hysteresis loop which runs far enough into saturation.

The drawbacks are: identification of parameters is difficult, the behavior of the model near loop tips is not physical and minor loops are not closed if saturation is not reached. The last drawback is a major obstacle for the use of this model in actual arbitrary network computations.

2.2 Models based on Preisach's Theory

Another approach for simulating hysteresis has relied on Preisach's theory [7], which assumes that the ferromagnetic material consists of magnetic dipoles that have a magnetization characteristic defined by two statistically distributed parameters h_c and h_m.

The model is able to generate the B-H trajectories without resorting to empirical definitions. The input data required for the model is the extrado function, which is the upper bound of the limiting hysteresis loop.

The theory assumes that the ferromagnetic material is made up of elemental dipoles in the B-H plane (Figure 2-1), may be described by coercivity h_c and field h_m due to neighboring dipoles. The parameters h_c and h_m are statistically distributed. Each elemental dipole may contribute either B_s or $-B_s$ to the total flux density B in the material.
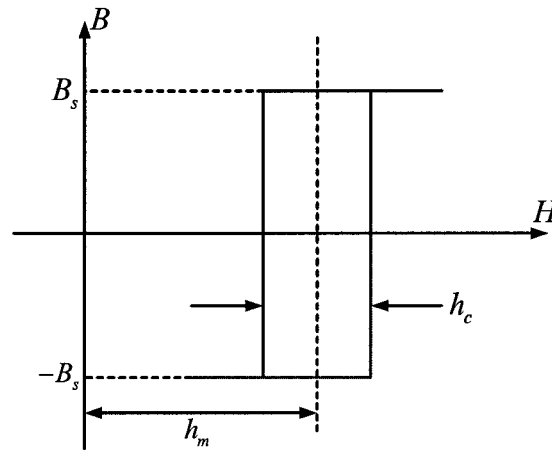
Figure 2-1 Magnetization characteristic of element dipoles

A probability density function is governing the distribution of elemental dipoles over the B-H plane. This determines the shape of the hysteresis and saturation functions by controlling the number of dipoles brought into alignment by incremental changes in

the field. For instance, if the probability density function is uniform, minor loops are predicted to assume a parabolic shape.

This model requires an efficient algorithm for computing the resultant field due to contributions from all dipoles. Agreement between predictions and field measurements is impressive, displaying the characteristic upward and downward trajectories including saturation and minor loops. Unfortunately its implementation is complex and may not be easily incorporated into simulation programs. Furthermore it is computationally inefficient for a large scale transient analysis application.

2.3 Macroscopic models

Models belonging to the third category make no attempt to associate observed behavior with physical phenomena. Empirical postulates are substituted in place of the more structured numerical method utilized by Preisach models to track magnetic states. The model is therefore more flexible, and computationally less demanding. It is likely adequate for practical studies since nonlinearities are difficult to characterize accurately in any event. The empirical approach is also consistent with the most commonly used EMTP models (Type-96 and 92 hysteretic reactors), which attach no physical significance to the non-linearity.

3 Available models in EMTP-V3

EMTP-V3 was the EMTP software version available prior to the new EMTP-RV development. Before starting the implementation of a new model in EMTP-RV it was obvious that the previously existing models had to be studied.

The use of digital computers to analyze transients in electric power systems requires accurate and efficient simulation models of all major pieces of equipment. Good models exist for transmission lines, synchronous machines and motors but a transformer model with accurate and realistic representation of the effects of the steel core has been lacking. A good transformer model is needed not only because transformers exist at every points in electric power systems where a change in voltage level takes place, but even more importantly because often transformer behavior is crucial to the phenomena being investigated.

Efforts in digital modeling of transformer non-linearities appear to concentrate in treating saturation and hysteresis as inseparable phenomenon. Reference [8] describes a usable concept of separate hysteresis and saturation effects.

3.1 The most commonly used model in EMTP : Type-96 hysteretic reactor

3.1.1 Theory of the Type-96 hysteresis model available in EMTP-V3

The modeling choice was based on the following criteria: conceptual simplicity, care of implementation within EMTP and demand on computer core memory. The original model is explained in [10] and its implementation details in EMTP are given in [3].

The minor loop trajectory of a hysteretic element can be defined in terms of its major loop. All points of operation are assumed to be within the major loop. The points beyond which the characteristic becomes single-valued are defined as the positive and negative saturation points (Figure 3-1).
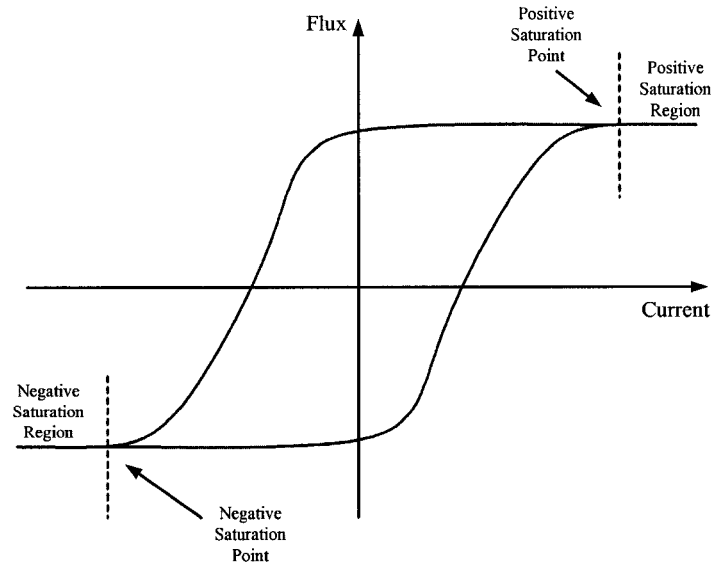
Figure 3-1   Typical major hysteresis loop characteristic

It is commonly assumed that after a flux reversal, the increasing flux trajectory passes through the previous-to-last reversal point.

Various points used in defining a minor loop trajectory are shown in Figure 3-2 for a trajectory created subsequent to a flux reversal at point 2. Φ_{rev} and I_{rev} are the flux and the current coordinates of the reversal point. D_{rev} is the vertical distance (always a positive value) between the reversal point and the major loop. Φ_{pt1} and I_{pt1} are the coordinate of the previous-to-last reversal point (point 1). The vertical distance between point 1 and the bottom half of the major loop is D_{pt1}. It is assumed that the vertical distance, D_{Φ}, between the major and minor loop trajectories decreases linearly with Φ. Specifically, by requiring that $D(\Phi_{rev}) = D_{rev}$ and $D(\Phi_{pt1}) = D_{pt1}$ it is possible to constrain a minor loop trajectory to pass through the previous-to-last reversal point.
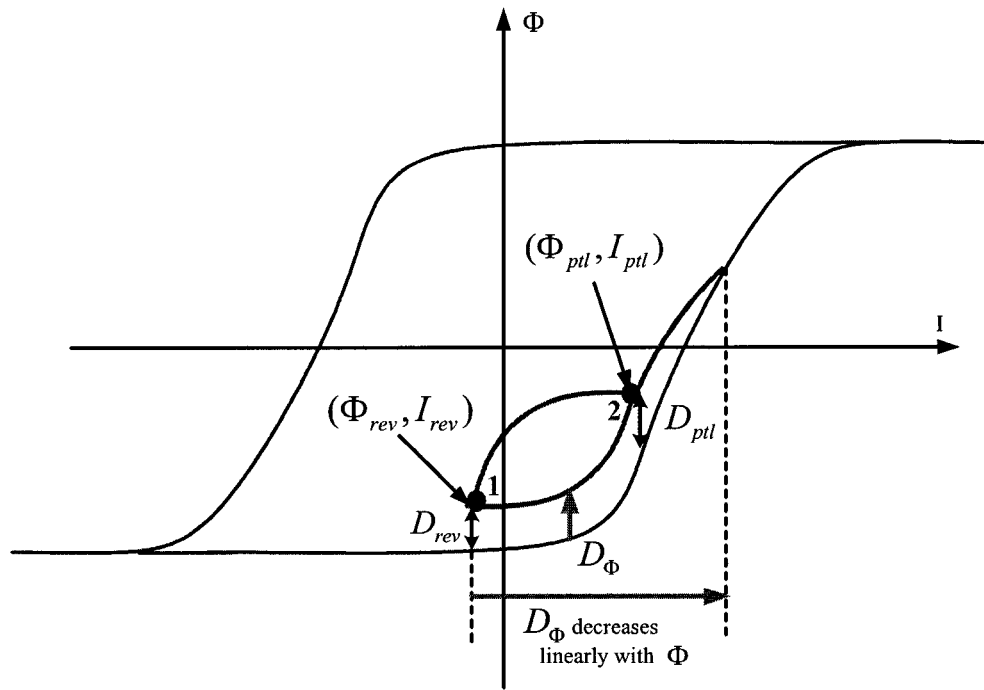
Figure 3-2   Creation of minor loop trajectory

It should be noted that this procedure describes the modeling under normal operations. Certain conditions require special handling. For instance, if the previous-to-last reversal point occurs in the saturation region, the trajectory subsequent to the reversal point would, under normal assumptions, goes outside the major loop. To eliminate such an illegal operation, whenever the reversal point occurs in the saturation region, the saturation point, rather than the actual point of reversal, is retained for the subsequent calculations.

3.1.2 Theoretical problems of Type-96 model

Several modifications have been made [9] to the original model described in [10] in order to match experimental results. However the model has been shown to remain at variance with the experimental results presented in [9] [5]:

- The existence of a "saturation point" is in doubt. A change in scale would probably show the major loops overlapping at a new point.

- In the unsaturated region, the curve shape following a reversal is independent of flux or current offset.

- More "history" of the device could be provided by storing reversal points older than the previous to last reversal point. Actually the trajectory "target" is more than the previous-to-last reversal point, it is the second-previous "active" reversal point K. Once K has been overtaken, the significance of the points K and K+1 is lost and an older reversal point becomes "active".

In Figure 3-3, the Type-96 model is caught out: after point 3 is overtaken, point 2 and point 1 have already been discarded and point 5 (positive saturation point) is the target. As a consequence "Minor loop 1" is open. In accordance with experimental results, after point 3 is overtaken, point 1 should have been the new "active target".
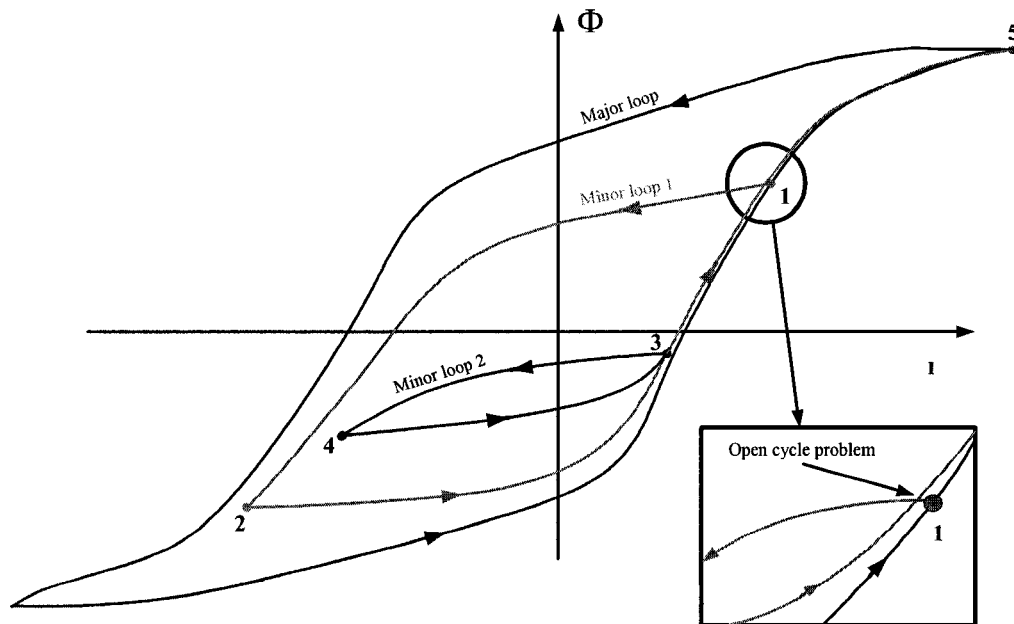
Figure 3-3   Open cycle problem the Type-96 model

3.1.3 Numerical methods in EMTP-V3 lead to problems for the Type-96 hysteretic reactor

In addition to physical modeling assumptions the Type-96 implementation was based only on the pseudo-nonlinear solution method of EMTP. This method converts the hysteresis slopes into a Norton equivalent which represents the relation between voltage and current at the given operating point and simulation time. Since there are no iterations it cannot be qualified as a simultaneous solution. The program changes operating segments only after illegally operating outside the range of the previous segment for one time-step. This results into the typical noisy behavior shown in Figure 3-4. The integration time step can be reduced to minimize such problems, but its drawback is to dramatically increase the simulation time.
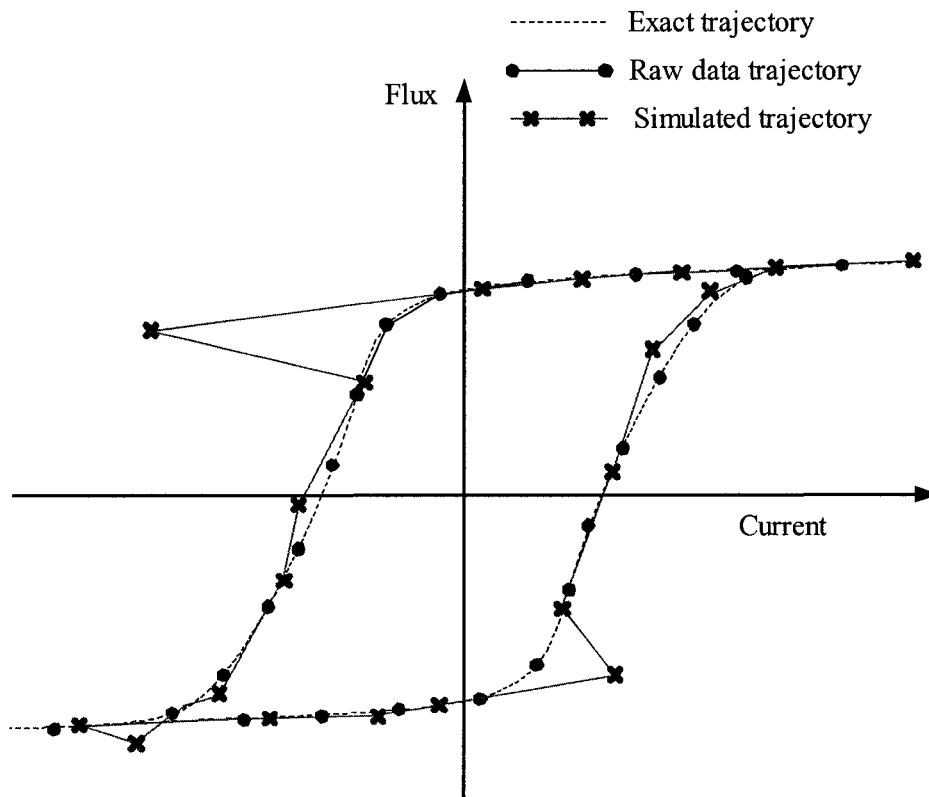
Figure 3-4 Pseudo-nonlinear model EMTP-V3: change of segment after illegal operation

3.2 Type-92 hysteresis model available in EMTP-V3

In addition to the Type-96 model, EMTP-V3 has the Type-92 model [4]. This model is classified as a true-nonlinear model and therefore has the inherent ability to achieve a simultaneous solution with network equations. It must be stressed however that this statement is true only under certain specific conditions.

This model is classified as a true-nonlinear model and therefore has the inherent ability to achieve a simultaneous solution with network equations. It remained however prone to numerical problems and limitations mainly due to the applied solution method for true-nonlinear models.

EMTP-V3 uses nodal analysis combined with the compensation method for the solution of the nonlinear functions. This method is presented in [12] and has been used for modeling nonlinear devices in EMTP-V3. It was designed to reduce the computer time required to solve nonlinear functions using the Newton method. It avoids the refactorization of the main linear system matrix by iterating with a reduced Thevenin equivalent derived from the linear network. The work presented in [13] has demonstrated that this method has several major disadvantages:

- It is extremely complicated to implement for solving several different types of nonlinear functions in the same subnetwork. An EMTP subnetwork is created due to time-domain decoupling by transmission line models. This means that in EMTP-V3 the nonlinear hysteretic model could not be combined with nonlinear inductance model or some nonlinear arrester models. This is a major problem in simulations, where the program user is forced to make changes which are irrelevant to the conducted study.

- The compensation method uses a Thevenin network equivalent where a voltage source vector and a resistive impedance matrix are used for representing the network surrounding the nonlinear device. The Thevenin network is derived from the linear network solution. The nonlinear device function is solved using the Newton method. The Jacobian matrix is explicitly derived. In addition to

topological restrictions (explained in the following bullet), this approach is prone to numerical problems and has poor convergence characteristics.

- In the compensation technique, the Thevenin impedance matrix imposes topological restrictions. Figure 3-5 shows some of typical topological restrictions with the compensation method: nonlinear devices cannot form a loop and cannot be connected in parallel with a voltage source.
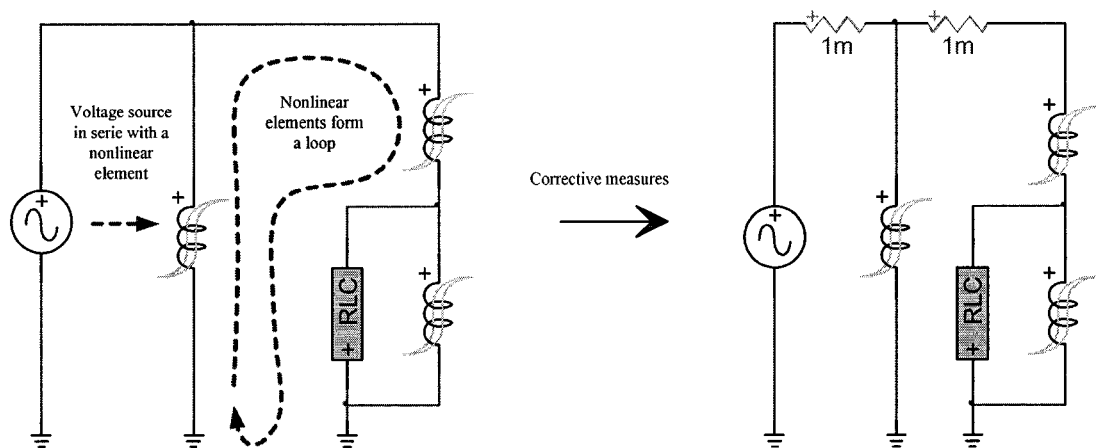
Figure 3-5   Illegal interconnections of nonlinear branches in EMTP-V3

The work presented in [15] has modified completely the methods used for solving nonlinear functions in time-domain. It has created a new computational environment for nonlinear device functions. All previously available limitations have been eliminated and the numerical robustness has been significantly increased. This new environment required revisiting the theories and programming of all nonlinear devices. The hysteretic reactor is one of these devices.

The following section presents the theory of the new model. This model follows the roots of the one utilized in the Type-92 element but that is the only overlap. The rest is a completely new and different contribution. The material also provides a complete

and not previously available document on the assumptions and detailed equations of the model.

After explaining the mathematical / numerical formulation of the model, this document presents its implementation into EMTP-RV. The numerical implementation is the major contribution and innovation of this work.

4 Theoretical background on the implemented model

4.1 Measurements of transformer characteristic.

Experimental results presented in reference [5] are used to develop this model. A low power test method has been used to obtain the instantaneous magnetization characteristics of large transformers. At lower currents, the described method also permitted observation of the behavior of minor hysteresis loops through reversal of the excitation. The results show that hysteresis curves tend to follow a certain simple relationship from which the new model will be derived. This test was carried on with cycling a laboratory model transformer through various hysteresis loops. With the proper scale adjustments, the results showed no practical differences with high power transformers.

Figure 4-1 shows a set of curves obtained on the laboratory transformer with scales adjusted to those of a 25 MVA unit. Test method for measurement of transformer characteristics is explained in [5].The current was first cycled to relatively large values (about 0.01 pu) to define the major loop. Beginning at point 1, the current was then cycled at decreasing levels to a final reversal at 9 followed by a large positive increase.
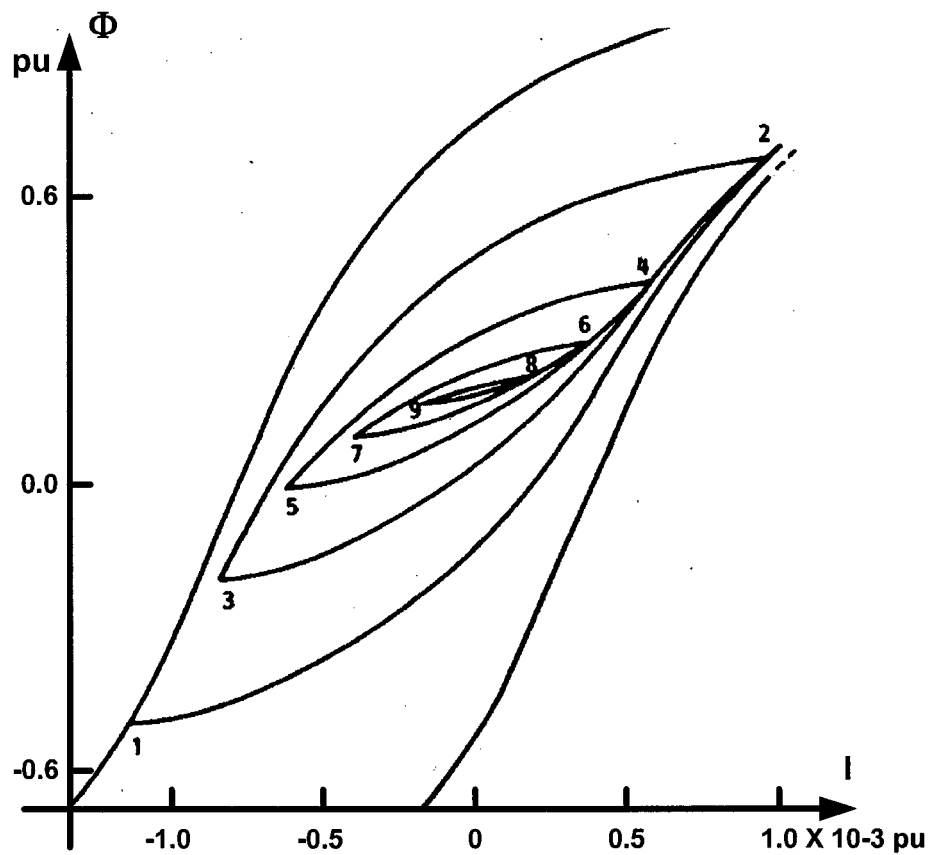
Figure 4-1   Magnetization curve at low current showing minor hysteresis loops

Several observations can be made from this figure:

- The shape of the magnetizing curve following a reversal appears to fit a simple template orientated either up or down, with a reference point on the template superimposed on the reversal point.

- Due to symmetry, each curve tends to return to reversal point previous to the last. For example, after point 9 the curve returns to point 8.

- Immediately upon overtaking a former reversal point, the template is shifted to a position defined by the next previous reversal point. For example, during the final increase in current and after overtaking point 8, the curve reverted to being defined point 7. Closer inspection of the figure confirms a step change in slope

on the final curve at point 8. Following a similar process, the curve then passed through point 6, point 4, and point 2 with a step change in slope at each.

- The loops converge to a non-zero flux linkage between point 8 and point 9 which depend on the location of the first reversal at 1. Thus the symmetry of minor loops is not necessarily aligned with that of the major loop.

- The remanence is not sufficient to specify the magnetization curve. For example, if point 9 had been the starting remanent point, developing the curve for increasing current would have required a knowledge of the previous reversal point.

These observations are limited to static hysteresis effects independent of excitation frequency.

4.2 Basic principles of the model

4.2.1 Hysteresis modeling

According to Reference [11] hysteresis is postulated to be the composite effect of an infinite number of infinitesimal "deadband" units while saturation is the combined effect of an infinite number of "hard limit" units. In each case, the units have sizes that distribute randomly within a definable statistical distribution.

Modeling of a laminated steel transformer core involves an input-output relationship between current driving the core and the resulting flux. Hysteresis appears to be a multi-valued function of current. Given a current, several values of flux seem to be possible. However, given an history of where current has been, flux is determinable. Saturation, on the other hand, is independent of history. The two effects are postulated to combine in series. The input to the saturation function being the output of the hysteresis function. The relationship between these two effects is very important.

Simple deadband or backlash is experience in several types of problems. Thinking in terms of an input/output relationship, output follows the input as long as input continues to move in the same direction. When the input reverses direction, the output follows the input again (Figure 4-2).
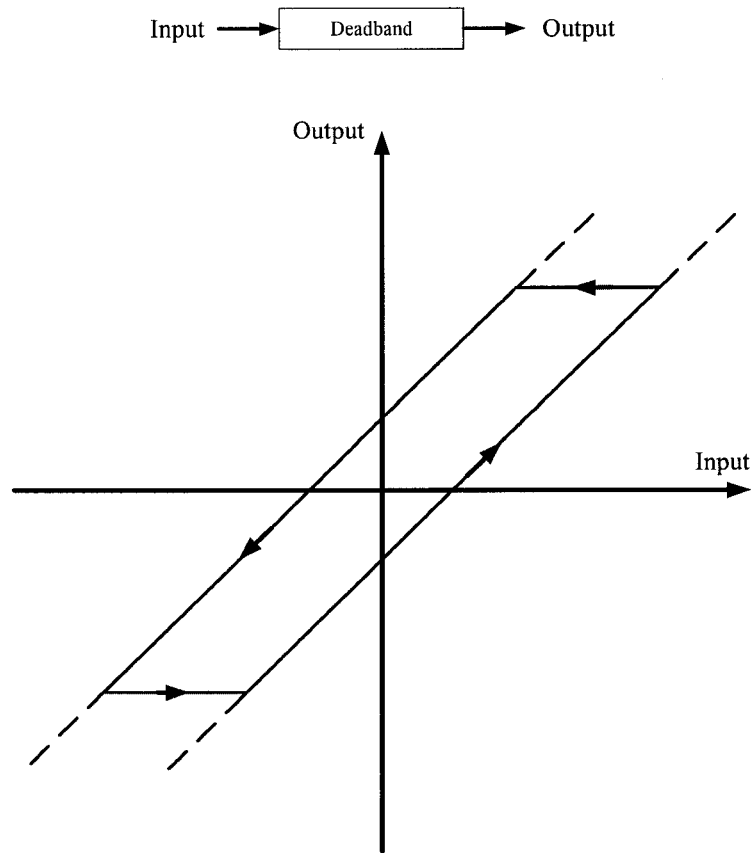
Figure 4-2   Input-Output properties of deadband

Hysteresis is very similar to deadband. The input is current and the output is flux. The only conceptual difference between simple deadband magnetic hysteresis is that hysteresis is the composite effect of a very large number of very small units; each small unit contributing its share to the input-output relationship. The units form a random distribution.

From a modeling standpoint, it is not practical to keep track of a large number of separate deadband units. Fortunately, that is not necessary. By modeling the shape of the curve that would be generated by an infinite number of infinitesimal units distributed according to given statistics, and keeping track of a limited number of reversal coordinates, an accurate model has been developed.

Several statistical distributions are shown on Figure 4-3 starting at the top with the elemental deadband units. f(x) represents a probability density function of elemental units. Its integral, F(x), represents the cumulative probability function. H(x), the integral of F(x), represents the cumulative effect of the elemental models and is the basic hysteresis input-output curve.
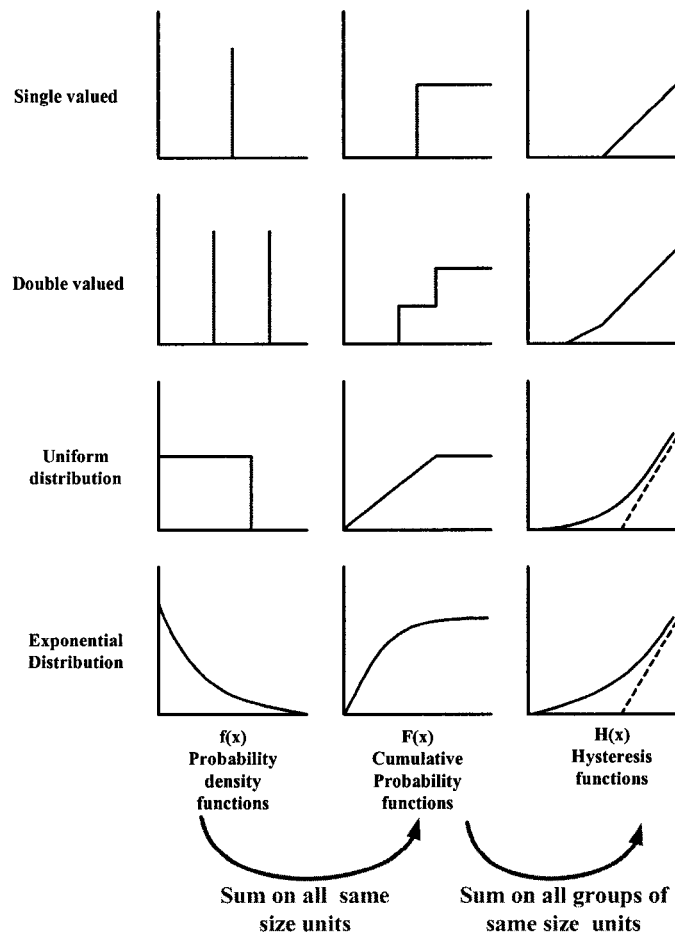
Figure 4-3 Candidate hysteresis functions

For convenience in modeling, the composite hysteresis effect is assumed to have a width of W ampere-turns with W depending on the core material and geometry. With this assumption, a universal hysteresis effect can be modeled with a width of 1 and an input-output slope of 1, then scaled later for the proper units.

The probability density function, f(x), can be selected such that h(x) matches any given hysteresis curve. The only constraints are :

- F(x) must approach or equal 1 for large x. This means that the integral of f(x) for current ranging from 0 to infinity must be 1.

- H(x) must be asymptotic to the curve x-1. This means that the mean of f(x) must be at x=1.

With these constraints, and by choosing an appropriate starting point, H(x) forms the right upward moving side of the hysteresis curve. Figure 4-4 shows how to model hysteresis with this theory.
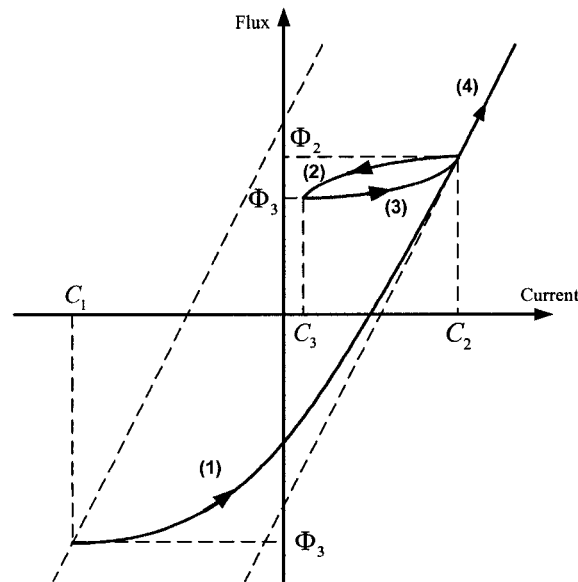
Figure 4-4   Illustration of elemental deadband units effects to create hysteresis shape

Current has started with some large negative value C_1 and steadily increased to C_2 along path 1, taking out all the deadband so that the output, Φ_2, equal $C_2 - \frac{1}{2}$. At this point, let current reverse direction. Since all the deadband units had been removed, each of the infinitesimal deadband units now must traverse its full width before contributing to a change in output. The downside function is simply the upside function flipped over

and path 2 will be traversed. Let current continue down to C_3, and again reverse. Now only the smaller elements have traversed their entire deadband. The larger elements have traversed only partially. All those small elements that had completely unwound their deadband will have to go back through in the other direction as current steadily increases. Path 3 will be traversed. When current reaches C_2, exactly the same elements that had unwound along path 2 will unwound again. Those that had only partly unwound along path 2 will have backed out of deadband completely at C_2. Thus all units are out of deadband and further increases in current will result in traversing path 4.

Notice that the transition from path 3 to path 4 involves a sudden change in slope. This phenomenon is exactly what happens in nature, but has not been accurately represented in some simulation models. The sudden change in slope will induce a change in voltage in linked windings so it is important to model this effect correctly.

The hysteresis model thus requires the equation for H(x), a reversal point stack in which to store coordinates of reversal points, knowledge of the direction current (or flux) is moving, whether current (or flux) has reversed direction since the last evaluation.

4.2.2 Saturation Modeling

This "pure hysteresis" modeling tends to represent the shape of minor loops. The shape of minor loops does not depend on the intensity of flux and current. If no reversal point appears, the hysteresis trajectory will follow the asymptote with no curvature. That is why saturation must be added to this model.

Input to the saturation function is the output of the hysteresis function. The saturation function is a single input, single output relationship between current and resulting flux, with the hysteresis effect removed.

Just as hysteresis was built up from elemental units of deadband, saturation is built up from elemental units of "hard limits" The phenomenon of magnetic saturation can be thought of as consisting of an infinite number of infinitesimal units, with individual magnitudes forming some statistical distribution.

Having gone through in detail how to go from elemental deadband units to a hysteresis model, it is sufficient to say that the same thinking can be applied to generate a distributed hard-limit saturation model

In the same way than hysteresis modeling thinking in terms of an input/output relationship is used to model saturation effect. The output is constant as long as the input is smaller than a value named L_{sat} (Figure 4-5).
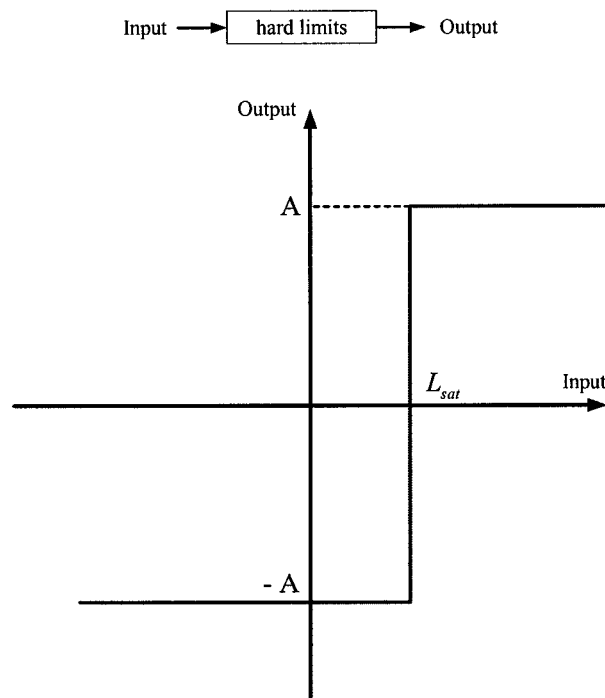
Figure 4-5   Input-Output properties of hard limits

Figure 4-5 can be compared to Figure 4-2 (Input-Output properties of deadband). A parallel with the previous hysteresis theory is done : the only conceptual difference between simple hard limits and magnetic saturation is that saturation is the composite effect of a very large number of very small units; each small unit contributing its share to the input-output relationship. The units form a random distribution. The constant L_{sat} of each unit are statistically distributed.

Depending on the statistical distribution of L_{sat} constant, the shape of the saturation curve is found (Figure 4-6)
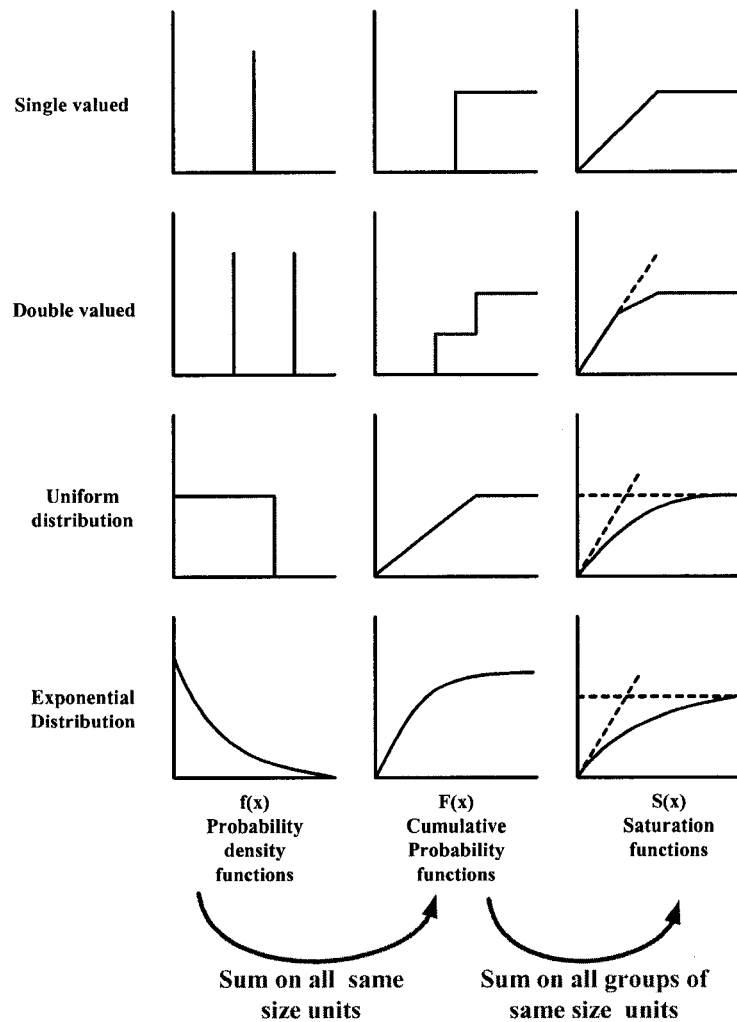
Figure 4-6   Candidate saturation functions

To form a complete hysteresis-saturation function, the two functions are simply put in series to form current versus instantaneous flux. Now the challenge is to choose simple functions to model saturation and hysteresis shape.

4.3 Modeling details

From the previous presentation it appears that minor hysteresis loops are part of a uniform template. Such a template may be constructed from an algebraic function.

The usual hysteresis models do not describe the real behavior of a magnetic material. They don't reproduce conveniently the come back to the saturation, the closing and the forgetting of secondary cycles.

These properties are however necessary in a correct transient simulation of power transformers to model their behavior in case of inrush, of internal or external faults and of chopping.

With regard to experimental hysteresis curves or to complex evolutions of the fields for materials used in power systems, the following properties apply in the i-φ map:

- symmetrical behavior
- closing and forgetting of the secondary cycles
- evolution is only a new trajectory function of the current point and of the last saved extrema

The hysteretic reactor is modeled by a closed-form function that relates instantaneous flux vs. current in two steps. An intermediate flux, named unsaturated flux, is used to link these two steps. Two different equations are also defined:

- A hysteresis function relating "unsaturated" flux λ_{unsat} to current. This function models the pure hysteresis effect: present state depends on previous state. Saturation is not taken into account: the more the current increases the more the intermediate flux increases.

- A saturation function relating instantaneous flux, named "saturated" flux λ_{sat}, to "unsaturated" flux λ_{unsat}. This function is to model the saturation effect: the more the input flux (unsaturated flux) increases the less the output flux increases.

Hysteresis and saturation functions are based on quadratic equations: modeled by hyperbolic branches. Only some parts of these branches are taken to obtain the final saturation curve.

4.3.1 Saturation modeling details

The following equation (4.1) and Figure 4-7 define hyperbolic asymptotes to straight lines $y_v = a_v x + b_v$ and $y_h = a_h x + b_h$:

$$C = (y_v - a_v x - b_v)(y_h - a_h x - b_h) \tag{4.1}$$
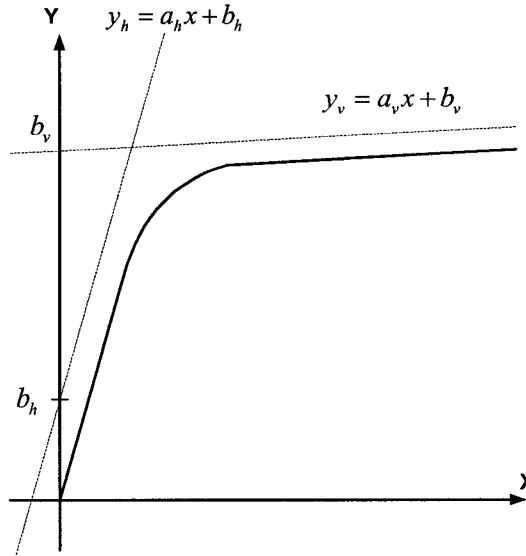
Figure 4-7   Hyperbolic template to model hysteresis and saturation

Parameter C defines the curvature of the curve, to control how close is the curve to asymptotes.

Firstly instantaneous flux (or saturated flux) is linked with unsaturated flux. The saturation equation (4.2) introduces saturation effect in the model.

$$C_{sat} = \left[\lambda_{unsat} - \frac{\lambda_{sat}}{S_{sv}} - X_{sv} \right] \left[S_{sh} \lambda_{unsat} - \lambda_{sat} + Y_{sh} \right] \tag{4.2}$$

This is a two variable quadratic equation with variables λ_{sat} and λ_{unsat}. When it is developed we obtain:

$$a \lambda_{unsat}^2 + b \lambda_{sat}^2 + c \lambda_{sat} \lambda_{unsat} + d \lambda_{sat} + e \lambda_{unsat} + f = 0 \tag{4.3}$$

Equation (4.3) can be divided into three parts. It is a multiplication of 2 terms defining the first two parts and C_{sat} is the third one.

The first two parts of this quadratic equation define 2 asymptotes. Equation (4.2) defines a hyperbolic function with 2 asymptotes : vertical and horizontal. The vertical asymptote defined by :

$$\lambda_{unsat} - \frac{\lambda_{sat}}{S_{sv}} - X_{sv} = 0 \qquad (4.4)$$

The equation of this asymptote is:

$$\lambda_{sat} = S_{sv}(\lambda_{unsat} - X_{sv}) \qquad (4.5)$$

It is a straight line with slope S_{sv} and x-axis intercept X_{sv}. The horizontal asymptote is defined by :

$$S_{sh}\lambda_{unsat} - \lambda_{sat} + Y_{sh} = 0 \qquad (4.6)$$

The equation of this asymptote is:

$$\lambda_{sat} = S_{sh}\lambda_{unsat} + Y_{sh} \qquad (4.7)$$

It is a straight line with slope S_{sh} and y-axis intercept Y_{sh}.

C_{sat} is the curvature of the curve. The smaller is C_{sat} the closer is the curve to its asymptotes. The influence of C_{sat} is demonstrated in Figure 4-8.
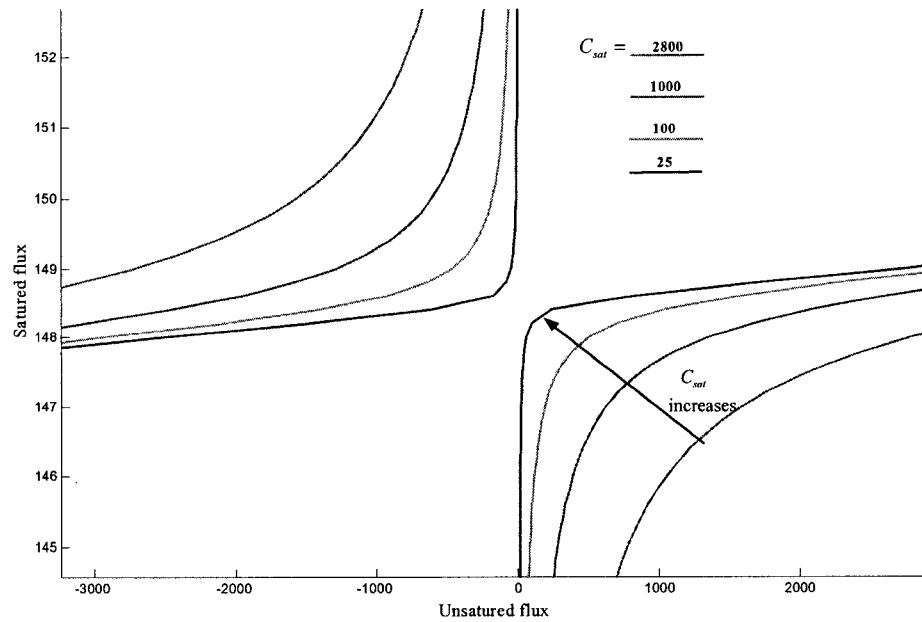
Figure 4-8   Curvature (C_{sat}) effect on shape of saturation curve

Asymptotes can be easily defined with their slopes and axis intercepts. A numerical example is given in Figure 4-9. S_{sh} is the slope of high saturation. It is related to the permeability μ_0.

Figure 4-9   Vertical and horizontal asymptote of the saturation curve

When the main shape of the saturation curve is defined, one branch will be chosen to be the final saturation curve. The concave branch will be taken for positive values of saturated and unsaturated flux. For negative values of flux, symmetry on the saturated branch is performed. As a consequence the final saturation curve passes through the origin (see Figure 4-10). No remanent flux is taken into account; it will be modeled with the hysteresis effect.
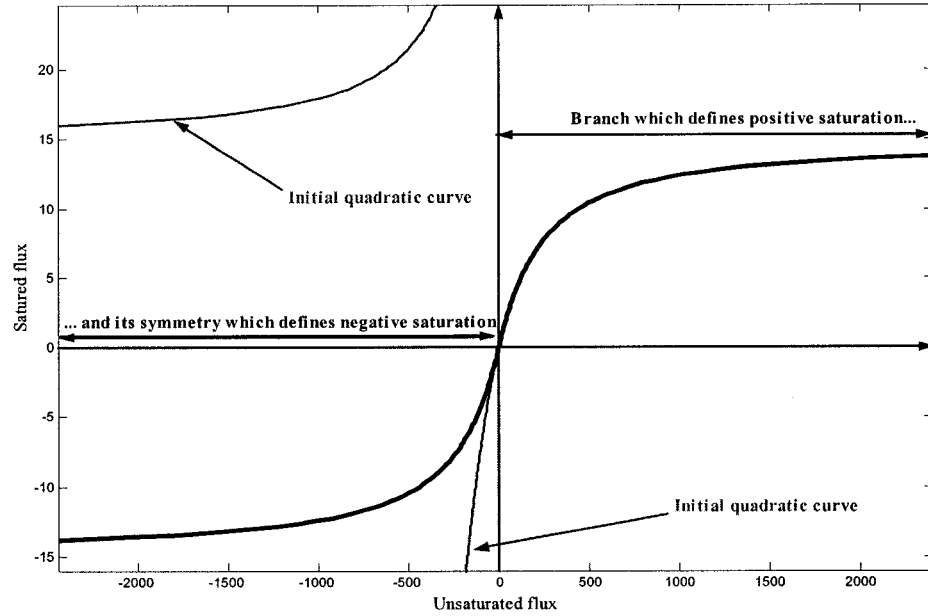
Figure 4-10   Final saturation curve

If unsaturated and saturated fluxes are equal to zero in equation (4.2) then C_{sat}

X_{sv} and Y_{sh} are linked with the following relation:

$$C_{sat} = X_{sv}Y_{sh}$$ (4.8)

Curvature of the saturation equation will be computed from this relation by the hysteretic fitter presented in a following chapter.

4.3.2 Hysteresis modeling details

The issue of modeling hysteresis is to find a relation between the instantaneous flux and the current in the transformer. In this model saturation and hysteresis are decoupled. We have seen that the saturation curve is represented by pieces of quadratic branches. It gives a link between the instantaneous flux, named saturated flux, and an intermediate flux, named unsaturated flux.

In the same way pure hysteresis is modeled with a quadratic equation (4.9) giving the unsaturated flux as a function of current.

$$C_{hyst} = \left[i - \frac{\lambda_{unsat}}{S_{hv}} - X_{hv} \right] [S_{hh} i - \lambda_{unsat} - Y_{hh}] \qquad (4.9)$$

This equation is of the same shape as the saturation equation. It is composed of 3 different parts. It is a multiplication of 2 terms defining the first two parts and C_{hyst} is the third one. The same remarks about the saturation will be done for the pure hysteresis equation.

The first two parts of this quadratic equation define 2 asymptotes. Equation (4.9) defines a hyperbola with 2 asymptotes: vertical and horizontal (see Figure 4-11). The vertical asymptote is defined by:

$$i - \frac{\lambda_{unsat}}{S_{hv}} - X_{hv} = 0 \qquad (4.10)$$

The equation of this asymptote is:

$$\lambda_{unsat} = S_{hv} (i - X_{hv}) \qquad (4.11)$$

It is a straight line with slope S_{hv} and x-axis intercept X_{hv}. The horizontal asymptote is defined by :

$$S_{hh} i - \lambda_{unsat} + Y_{hh} = 0 \qquad (4.12)$$

The equation of this asymptote is:

$$\lambda_{unsat} = S_{hh} i + Y_{hh} \qquad (4.13)$$

It is a straight line with slope S_{hh} and y-axis intercept Y_{hh}.

C_{hyst} is the curvature of the curve. The smaller is C_{hyst} the closer is the curve to its asymptotes.
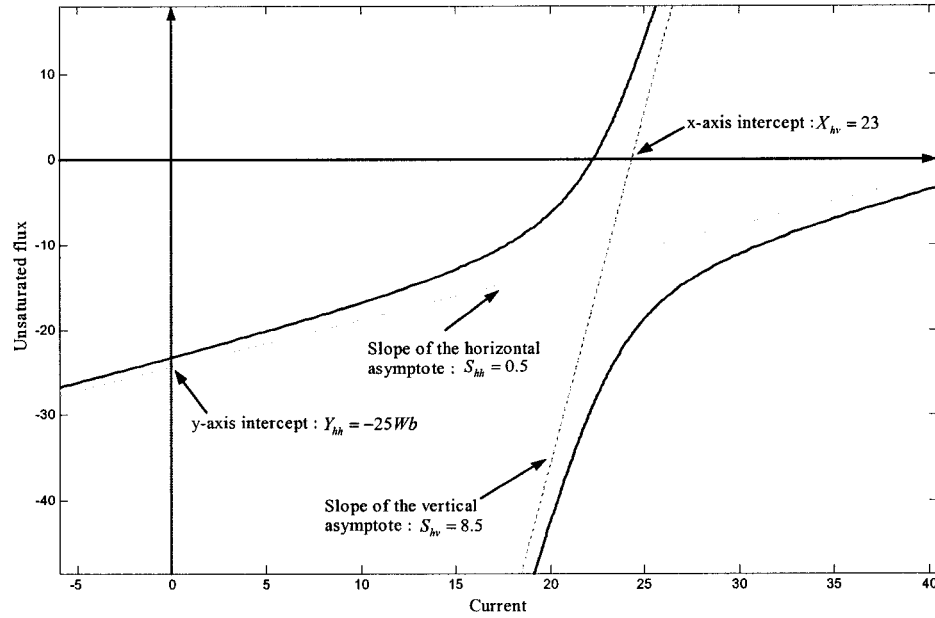
Figure 4-11 Vertical and horizontal asymptotes of the hysteresis curve
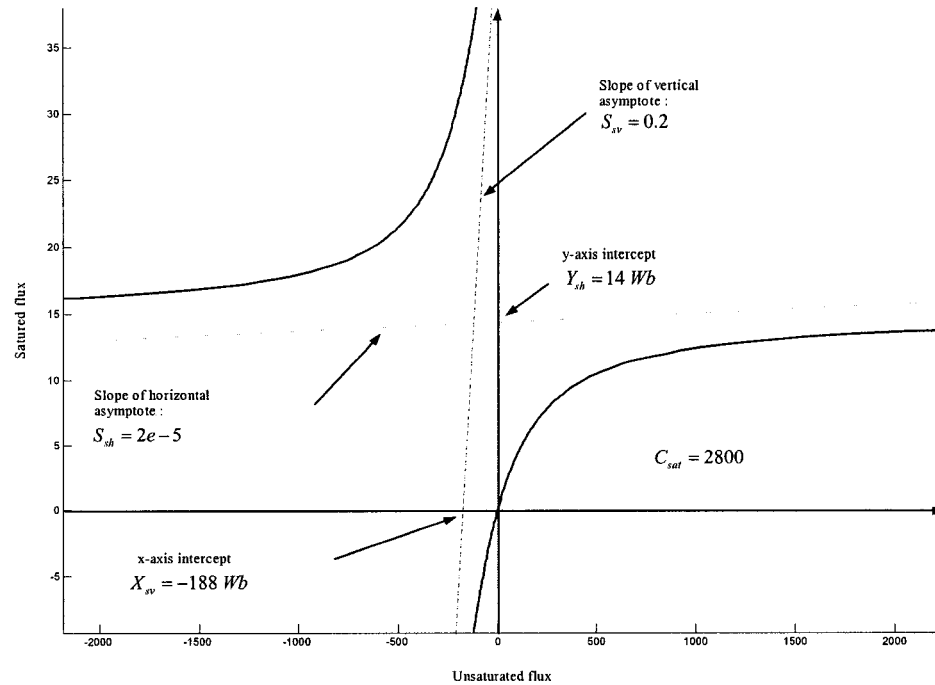
When the main shape of the hysteresis curve is defined, the convex branch will be chosen for upward trajectory and the concave for downward trajectory. But these two branches cannot define a closed shape. A translation of this hysteresis curve will give the width of the loop. To translate the curve we only have to translate the asymptotes. The slopes of the asymptotes do not change, but the axis intercepts will change their sign. As a consequence the translated curve is be defined by:

$$C_{hyst} = \left[i - \frac{\lambda_{unsat}}{S_{hv}} + X_{hv} \right] \left[S_{hh}\, i - \lambda_{unsat} + Y_{hh} \right]$$

(4.14)

Figure 4-12 shows the initial curve (solid blue line) and the translated curve (red dashed line). The upward and downward trajectories form the hysteresis loop.
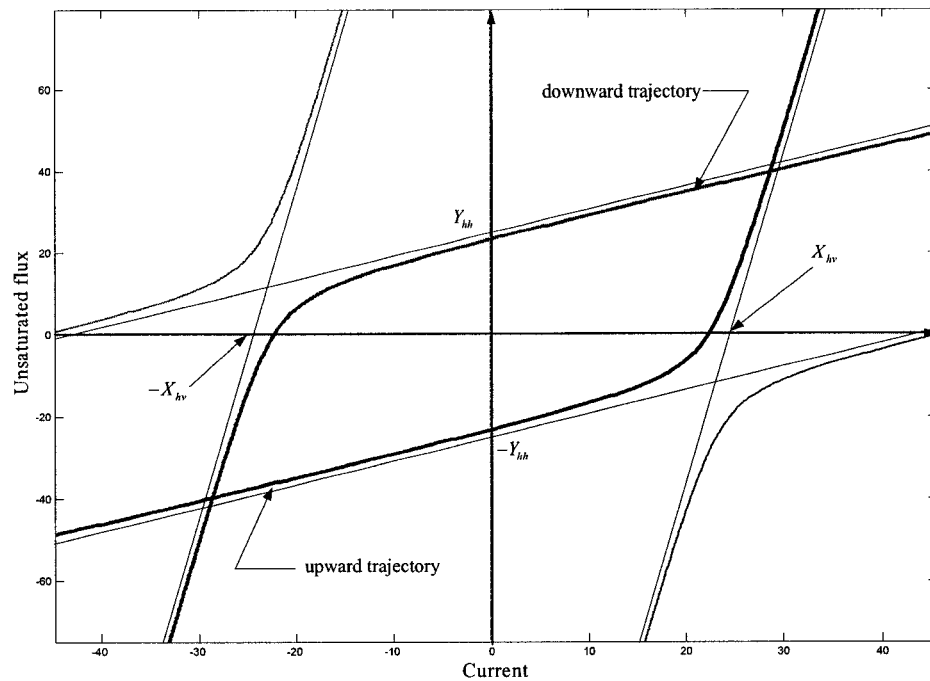
Figure 4-12 Translation of the main hysteresis hyperbola to obtain a closed loop

4.3.3 Modeling minor loops

Hysteresis trajectories are postulated to follow a uniform template, mapping current and unsaturated flux linkage λ_{unsat} (equation (4.14)). Upward and downward trajectories correspond to opposite template orientations, specified by selecting the appropriate root for the second order equation. Parameters X_{hv} and Y_{hh} control template position in the $\lambda_{unsat} - i$ map, hence they are modified systematically during simulation in accordance with the implemented model. As such, initially specified values are inconsequential. On the other hand, parameters S_{hh}, S_{hv} and C_{hyst} define template shape, which is fixed. Values for these parameters may be determined from recorded hysteresis loops.

When a reversal point is detected, a new trajectory begins. A reversal point occurs when the flux $\Phi(t + \Delta t) < \Phi(t)$ on an upward trajectory or when $\Phi(t + \Delta t) > \Phi(t)$ on a downward trajectory. Since template shape is independent of its position, the starting point for a trajectory (i.e. a reversal point) is chosen as the origin for the coordinate system. Then, in accordance with the postulated model, the vertical asymptote (slope S_{hv}) is displaced to the right along the abscissa (or left for downward trajectory) by a distance equal to twice the coercive current COER (Figure 4-13). A minor loop trajectory cannot exceed the major loop asymptote.
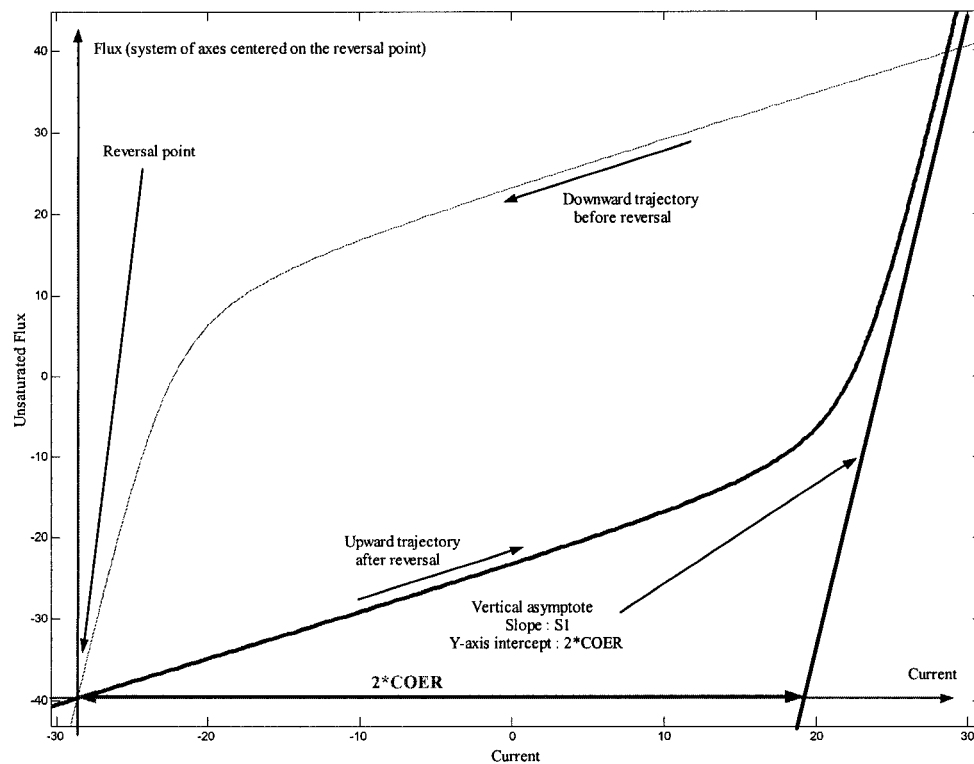
Figure 4-13   Positioning of template after flux reversal to direct return trajectory through the penultimate reversal point

The new trajectory passes through the origin of the new system of axes:

$$X_{hv} = \frac{C_{hyst}}{Y_{hh}}$$

(4.15)

Therefore the position of the horizontal asymptote is known (Figure 4-14).
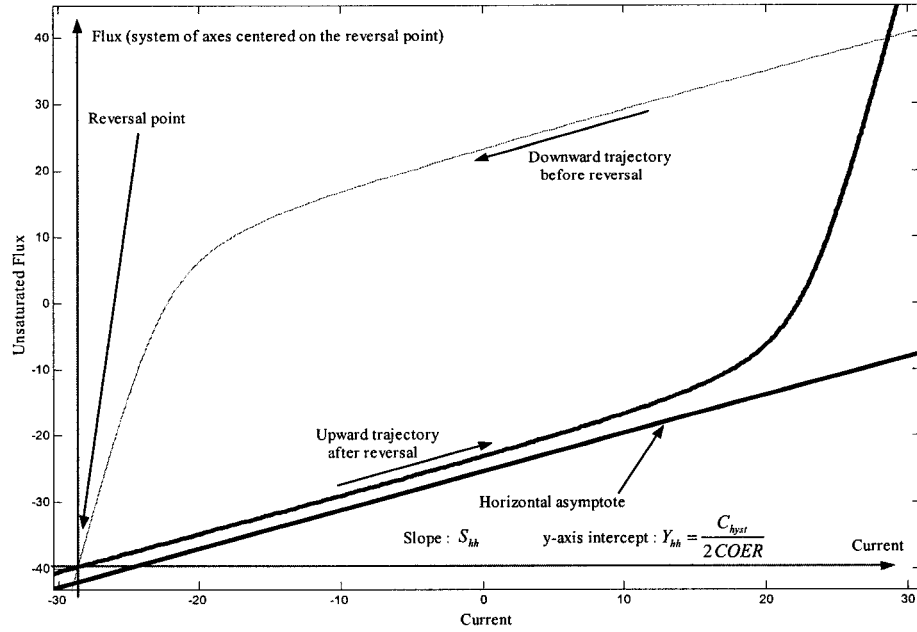
Figure 4-14 Position of horizontal asymptote

To come back to the old system of axes a simple translation of last reversal point is required. So axis intercept that defines shape of minor loop is given by template shape and last reversal point (x_{rev} , y_{rev}) :

$$X_{hv} = X_{rev} + 2 \ trajec \ COER - \frac{Y_{rev}}{S_{hv}}$$

(4.16)

and

$$Y_{hh} = -X_{rev} \, S_{hh} + Y_{rev} - \frac{C_{hyst} \ trajec}{2 \, COER}$$

(4.17)

With $trajec = 1$ for a upward trajectory after reversal point and $trajec = -1$ for a downward trajectory after reversal point.

When a system goes out of a minor loop it passes through the previous to last reversal point. Modeling with hyperbolic functions is powerful because they impose a symmetry that leads to closed minor loops. Nothing has to be added to close the minor loops: hyperbolic branches automatically pass through the previous-to-last reversal point.

The reversal points preceding the current loop must be saved. Figure 4-15 illustrates the progression from the inner loop A. When the flux increases beyond the reversal point 5, the reversal point that defines the trajectory is 4. That is why a reversal point stack composed of (λ_{unsat}, i) value pairs is used to save the reversal points out of the present loop.
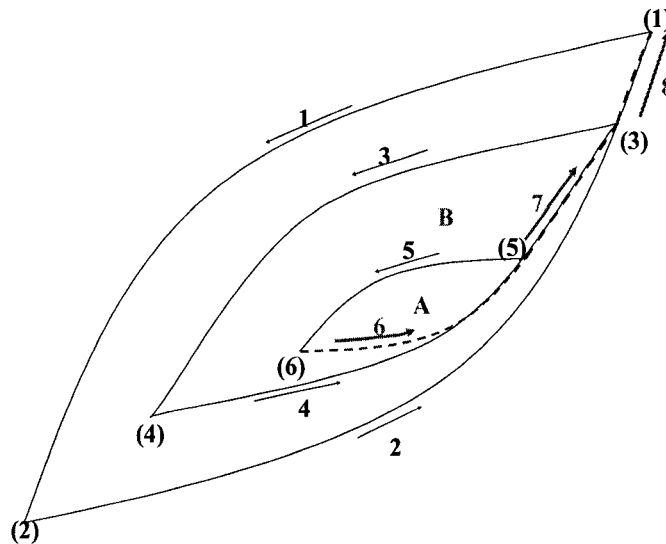
Figure 4-15   Reversal points in hysteresis trajectories

4.3.4 Initialization

Before starting the time loop solution, it is needed to initialize the reversal points stack. The first 2 points of this stack are initialized with very high flux (10^{10} Wb) for defining the borders of the major loop. The remaining variables depend on the type of initialization.

If 'manual' initial conditions (manual remanent flux Φ_0) are used then the initialization proceeds as shown in Figure 4-16. Point 2 (current i_2) is arbitrarily chosen for a current 50 times the coercive current. The next step is to determine equation (4.9) for a trajectory passing through Φ_0 which will give point 1. It is assumed that the trajectory between the last reversal point and Φ_0 is a downward trajectory if $\Phi_0 \geq 0$ and upward trajectory if $\Phi_0 < 0$. Such behavior is consistent with the deenergization pattern of a transformer. The point 2 is chosen sufficiently high to enable placing Φ_0 on the upper trajectory between 2 and 1 when $\Phi_0 \geq 0$ and on the lower trajectory when $\Phi_0 < 0$. If this condition is not satisfied then point 2 must be moved. The same technique is applicable to $\Phi_0 = 0$.
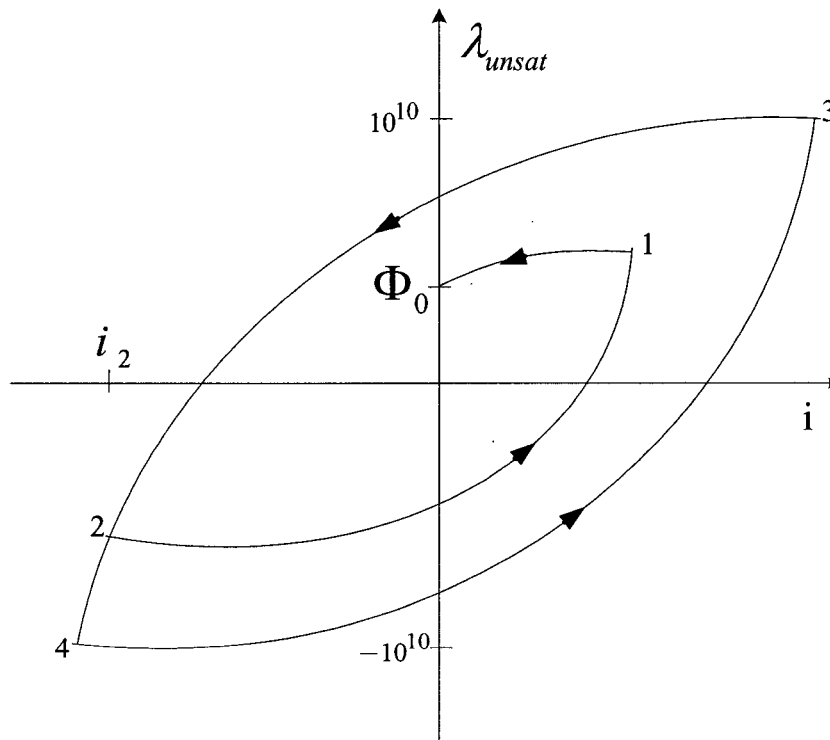
Figure 4-16   Reversal points stack for manual initial conditions

If it is chosen to connect the reactor during the steady-state phasor solution, one option is to use an inductance value taken from the slope of the major hysteresis loop at zero flux. In this case the initialization points are given in Figure 4-17. Points 3 and 4 are defined using $10\Phi_{ss}$. The choice of $10\Phi_{ss}$ (where Φ_{ss} is the flux at t=0 from the steady-state phasor solution) is again arbitrary, but has been found acceptable in most cases.
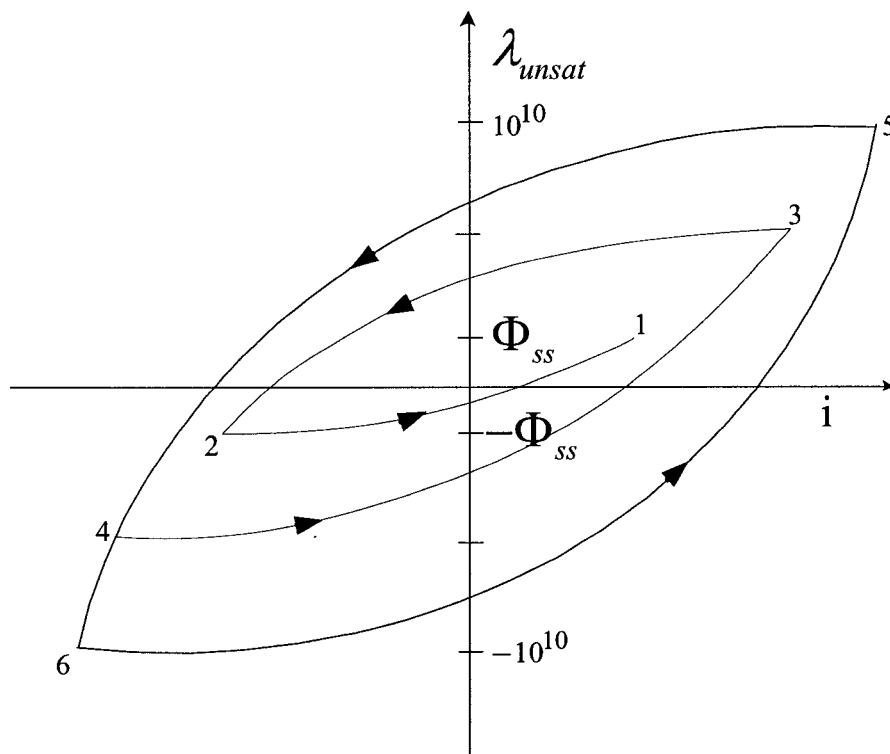
Figure 4-17   Reversal points stack initialization from steady-state

5 Implementation in EMTP-RV

The previous section has presented the mathematical formulation of the model. This section presents the actual numerical implementation in EMTP-RV. Numerical implementation in an industrial grade application has several challenges. The chosen method must be robust and must work in generic networks without particular considerations. A separate fitter for converting user data to model data has been also programmed.

5.1 The hysteresis fitter

The hysteretic reactor is defined by equations (4.2) and (4.9). As a first step it is required to provide a fitting method for determining the parameters of these 2 equations. Such a fitter and its formulation already existed in EMTP-V3 [14] but it remained prone to numerical problems. Assumptions and applied theories were obscure. That is why a new fitter subroutine has been developed in this project.

The purpose of this subroutine is to define equations (4.2) and (4.9) from the magnetizing curves of power transformers. Three types of data are used: saturation characteristic, parameters for minor loops shape and simulation parameters.

Hysteresis effect can depend on parameters that are not an input for this model. For instance, temperature dependence can be taken into account if the user has saturation characteristic for different temperatures.

5.1.1 Saturation characteristic fitting

Saturation (or magnetizing) characteristic of power transformer is used to find the saturation function parameters of equation (4.2). This equation gives the shape of the major hysteretic loop. The new fitter uses a least-squares method for finding these parameters. The parameter S_{hv} is also determined by this method since during the fitting process λ_{unsat} is replaced by $S_{hv}i$.

The fitting method used in the hysteresis fitter (named FITSAT-RV) is a least squares method. The fitting process must find the parameters:

- S_{sv} : vertical asymptote slope of the saturation equation defined in (4.2)

- S_{sh} : horizontal asymptote slope of the saturation equation defined in (4.2)

- Y_{sh} : y-axis intercept of the horizontal asymptote of the saturation equation defined in (4.2)

- X_{sv} : x-axis intercept of the vertical asymptote of the saturation equation defined in (4.2)

- S_{hv} : vertical asymptote slope of the hysteresis equation defined in (4.9)

The other parameters are found by an exact method. Before starting the fitting loop these parameters must be initialized as follows:

- $S_{sv} = 1$

- S_{sh} is taken as the slope defined by the last two points of input characteristic multiplied by S_{hv}.

- Y_{sh} is initialized with the y-axis intersection of the straight line defined by the last two points of input characteristic.

- S_{sh} is computed as follows : if there is no inflexion point before the saturation curvature, S_{sh} is initialized with the slope defined by the first point of input characteristic and the origin. If there is an inflexion point before the saturation curvature, S_{sh} is initialized with the mean slope of each segment before saturation curvature.

- X_{sv} is set to zero.

The fitting method minimizes the distance between raw data and a nonlinear function. This function is based on the above parameters. The nonlinear function F is defined by the saturation equation (4.2).

It is assumed that :

$$\lambda_{unsat} = S_{hv} i \tag{5.1}$$

The previous equation defines the vertical asymptote of the hysteretic curve. As a consequence λ_{sat} vs. current is given by:

$$\frac{C_{sat}}{S_{hv}} = \left(i - \frac{\lambda_{sat}}{S_{sv} S_{hv}} - \frac{X_{sv}}{S_{hv}} \right) \left(S_{sh} S_{hv} i - \lambda_{sat} + Y_{sh} \right) \tag{5.2}$$

and the nonlinear function $F(\lambda_{sat}, i)$ is defined by :

$$F(\lambda_{sat}, i) = \frac{C_{sat}}{S_{hv}} = \left(i - \frac{\lambda_{sat}}{S_{sv} S_{hv}} - \frac{X_{sv}}{S_{hv}} \right) \left(S_{sh} S_{hv} i - \lambda_{sat} + Y_{sh} \right) + \frac{X_{sv} Y_{sh}}{S_{hv}} \tag{5.3}$$

It is assumed that

$$C_{sat} = -X_{sv} Y_{sh} \tag{5.4}$$

since the saturation curve passes through the origin.

F is a vector of length equal to the number of raw data points. The fitting algorithm tries to find the best 5 parameters to minimize $\left\| F(\lambda_{sat}, i) \right\|^2$.

When previous fitting is done, saturation curve is completely known. The S_{hv} (hysteretic parameter) is also known. The other hysteretic parameters are now fixed by user supplied values Y_{rev}, $Slope_{rev}$ and (X_0, Y_0).

Y_{rev} is the reversal point y-coordinate of a given loop. It should not be zero. Then (X_{rev}, Y_{rev}) defines a starting point for a hysteretic trajectory. X_{rev} is chosen on the vertical asymptote. $Slope_{rev}$ is the slope at the reversal point (X_{rev}, Y_{rev}).

(X_0, Y_0) is a point on the trajectory beginning at (X_{rev}, Y_{rev}) and so it is a solution of the hysteretic equation defined by the previous reversal point (X_{rev}, Y_{rev}). This general hysteretic equation is equation (4.9).

As a consequence :

$$\left(X_0 - \frac{1}{S_{hv}} Y_0 + COER \right) \left(X_0 S_{hh} - Y_0 - Y_{hh} \right) = C_{hyst} \tag{5.5}$$

and :

$$\left(X_{rev} - \frac{1}{S_{hv}} Y_{revu} + COER \right) \left(X_{rev} . S_{hh} + Y_{revu} - Y_{hh} \right) = C_{hyst} \tag{5.6}$$

with:

$$C_1 = (X_{rev} - \frac{1}{S_{hv}} Y_{revu} + COER) \tag{5.7}$$

and :

$$C_2 = (X_0 - \frac{1}{S_{hv}} Y_0 + COER) \tag{5.8}$$

Equations (5.5)-(5.6) give :

$$X_{hv} = C_3 - C_4 S_{hh} \tag{5.9}$$

with :

$$C_3 = \frac{C_3 Y_{revu} - C_2 Y_0}{C_2 - C_1} \tag{5.10}$$

$$C_4 = \frac{C_2 X_0 S_{hh} - C_1 X_{rev} S_{hh}}{C_2 - C_1} \tag{5.11}$$

Moreover the differential of (4.9) gives :

$$(di - \frac{d\lambda_{unsat}}{S_{hv}})(i S_{hh} - \lambda_{unsat} - Y_{hh}) + (i - \frac{\lambda_{unsat}}{S_{hv}} + COER)(S_{hh} di - d\lambda_{unsat}) = 0 \tag{5.12}$$

The slope at (X_{rev}, Y_{revu}) is $Slope_{rev}$ so :

$$\frac{\partial \lambda_{unsat}}{\partial i}(X_{rev}, Y_{revu}) = Slope_{rev} \tag{5.13}$$

Finally (5.9), (5.12) and (5.13) give:

$$S_{hh} = \frac{C_6}{C_5} \tag{5.14}$$

with :

$$C_5 = \left(1 - \frac{Slope_{revu}}{S_{hv}}\right)(X_{rev} - C_4) + C_1 \tag{5.15}$$

$$C_6 = \left(1 - \frac{Slope_{revu}}{S_{hv}}\right)(-C_3 + \lambda_{unsat}) + C_1 Slope_{revu} \tag{5.16}$$

and :

$$Y_{hh} = C_3 + C_4 \frac{C_6}{C_5} \tag{5.17}$$

Equations (5.5) or (5.6) can be used to find C_{hyst}. Parameters for the hysteretic equation are determined completely. To change curvature or minor loop slopes, users have only to change Y_{rev} and $Slope_{rev}$ ($Slope_{rev}$ must be greater than S_{hv}, otherwise C_{hyst} is negative).

5.1.2 Saturation characteristic available in EMTP-V3

Saturation characteristics of power transformers are commonly available in EMTP–V3 data files to define Type-96 hysteretic reactor [3]. Most users will be inclined to use such data. An example of such a characteristic is given below for a 58 MVA power transformer. This is also typical data that can be available from measurements.

```
C Hysteresis reactor Type-96
C [BUS1][BUS2][BUS1][BUS2]<Iste><Phis><Prem>
C 3456789-123456789-123456789-123456789-123456789-
96LSATUARDNTSB              8888.      00.000
C <---Courant--><-----Flux----->
C coercitive current = 0.56 A
        -3674.60        -89.50
         -297.10        -80.18
         -171.60        -78.59
          -76.60        -73.85
          -38.20        -69.41
          -16.10        -65.15
           -7.80        -62.40
           -3.20        -59.28
           -0.60        -56.00
            0.05        -54.25
            0.30        -51.00
            0.50         51.00
            0.75         54.25
            1.40         56.00
            4.00         59.28
            8.60         62.40
           16.90         65.15
           39.00         69.41
           77.40         73.85
          172.40         78.59
          297.90         80.18
         3675.40         89.50
         9999.
```

This magnetization characteristic is actually the upward trajectory of the main hysteretic loop. Figure 5-1 is the plot of this data. The width of the major loop is not visible on this figure due to the selected scale.
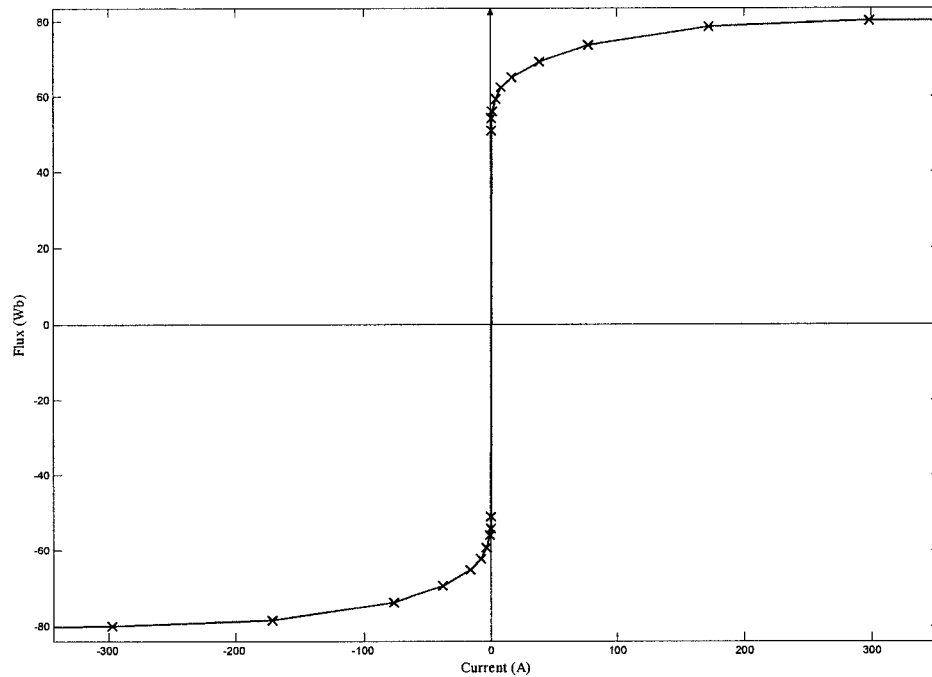
Figure 5-1   Example of saturation characteristic

5.1.3 Saturation characteristic for the new model

The new fitter assumes that the magnetizing characteristic is symmetrical for positive and negative fluxes [11]. As a consequence characteristic for negative fluxes is not used.

Optional input methods are available :

- the upward branch of hysteresis main loop (called "offset characteristic")

- the upward branch of hysteresis main loop passing through the origin (called "centered characteristic"). The half width of the major loop is defined by COER.

Figure 5-2 gives an example for these two options.

Magnetizing characteristic passing through the
origin : half width of the major loop is
manually defined by *COER* value

Flux

Magnetizing characteristic passing
through coercitive current at zero flux

Current

COER
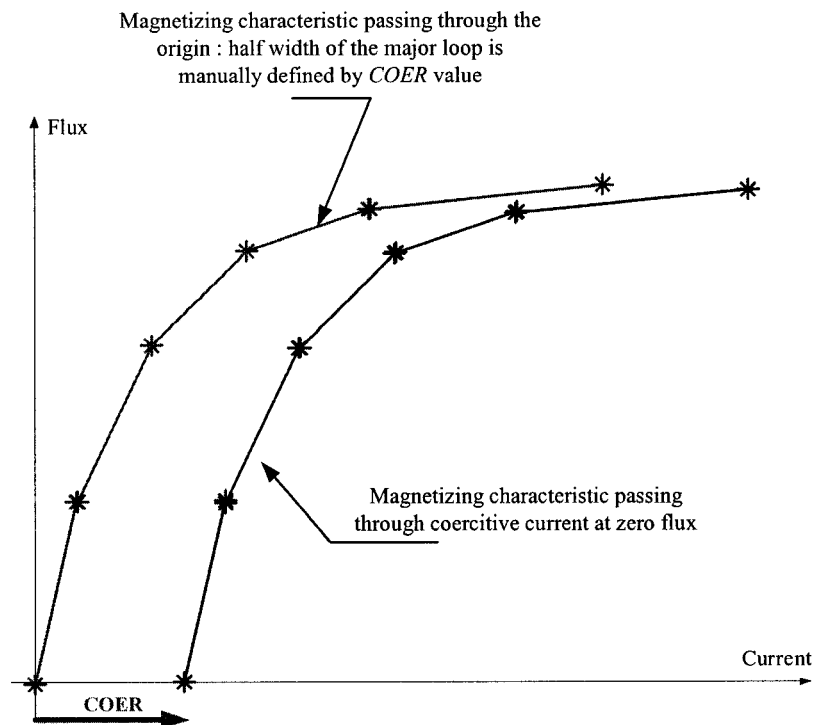
Figure 5-2   Sample saturation characteristics: 2 ways to define the same hysteresis loop

In the graphical user interface of EMTP-RV (EMTPWorks [2]) the user can find a hysteretic fitter device in the "nonlinear library" (Figure 5-3).

hfit1
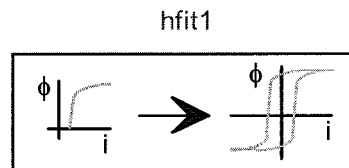
Figure 5-3   The hysteretic fitter device in EMTPWorks

Figure 5-4 shows the opening data panel when the user double-clicks on the above device. The saturation data presented above can be entered as shown in Figure 5-4.

Figure 5-4   The hysteretic fitter data form: saturation characteristic

5.1.4 Minor loop data

Minor loop shape is described by the hysteresis equation (4.9). Out of saturation area minor loop shapes are completely independent of saturation parameters. That is why the fitter needs minor loop data:

- y_{rev} : The y-coordinate of the reversal point of a given loop. y_{rev} should not be zero. Default is 5.0. The x-coordinate of the reversal point, x_{rev} is calculated by the program (when the user enters 0) assuming that the reversal point belongs to major loop (on the vertical asymptote).

- $Slope_{rev}$: Slope at the reversal point (x_{rev}, y_{rev}) Default is 5.0.

- y_0 : y-coordinate of a reversal point in a trajectory where the reversal point is given by (x_{rev}, y_{rev}) and $Slope_{rev}$. This point is, as a consequence, on the same hyperbolic curve than (x_{rev}, y_{rev}). Default is 0.

- x_0: x-cooordinate of a second point in a trajectory where the reversal point is given by (x_{rev}, y_{rev}) and $Slope_{rev}$. Default is 0.

When this data is not available, the provided default values have been tested for producing acceptable results in most cases. The user can modify the default data through the data entry form presented in Figure 5-4 and explained in Figure 5-5.
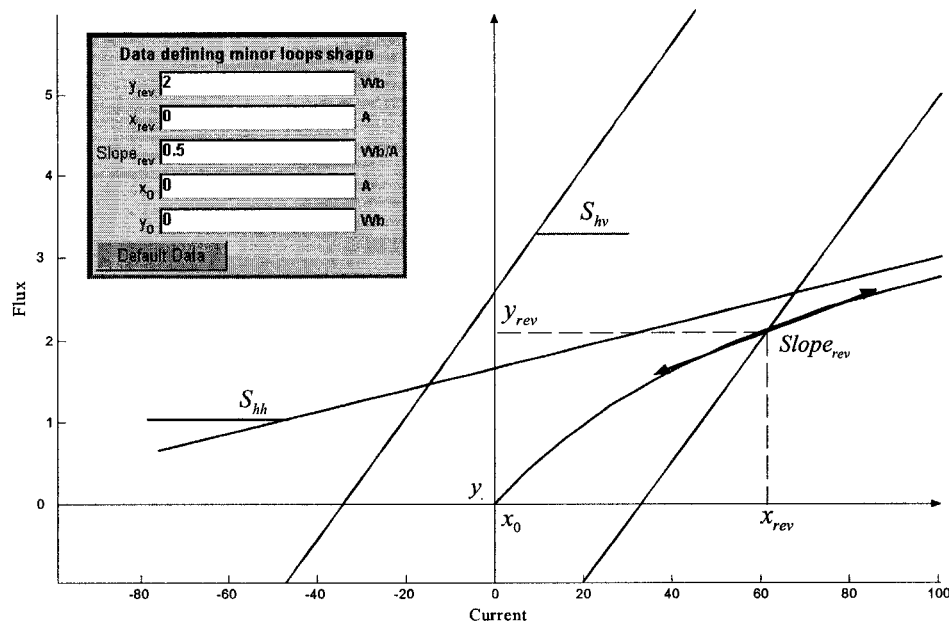
Figure 5-5   Data to model minor shapes

The choice of y_{rev} is important for determining the shape of minor loops. Simulations have been performed to see the effect of y_{rev}. They lead to the conclusion that y_{rev} must be chosen in the unsaturated part of the hysteresis loop. It is logical to have such a choice because y_{rev} is appropriate to model the minor loops in the unsaturated area. The comparisons have been carried out on the shape of minor loops. The reference was the

shape given by Type-96 hysteresis model (blue dashed line in Figure 5-6 and Figure 5-7). No other data was available.
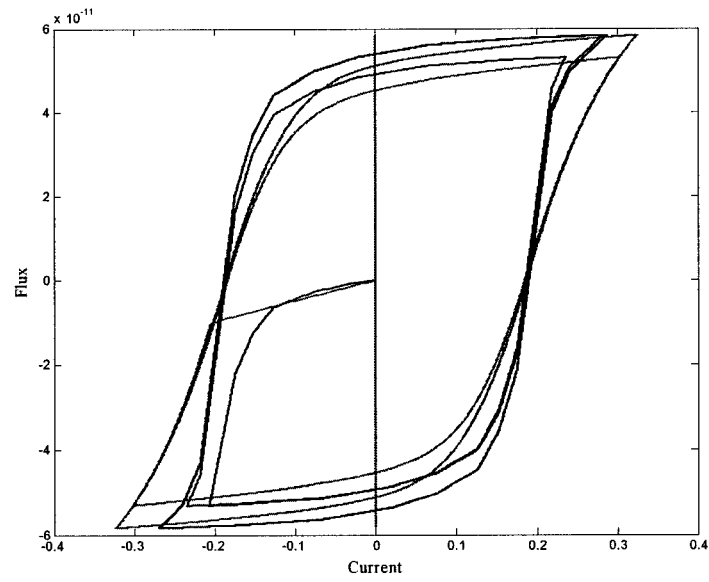
Figure 5-6   Effect of y_{rev} on the shape of minor loops : y_{rev} = 3% of maximum flux
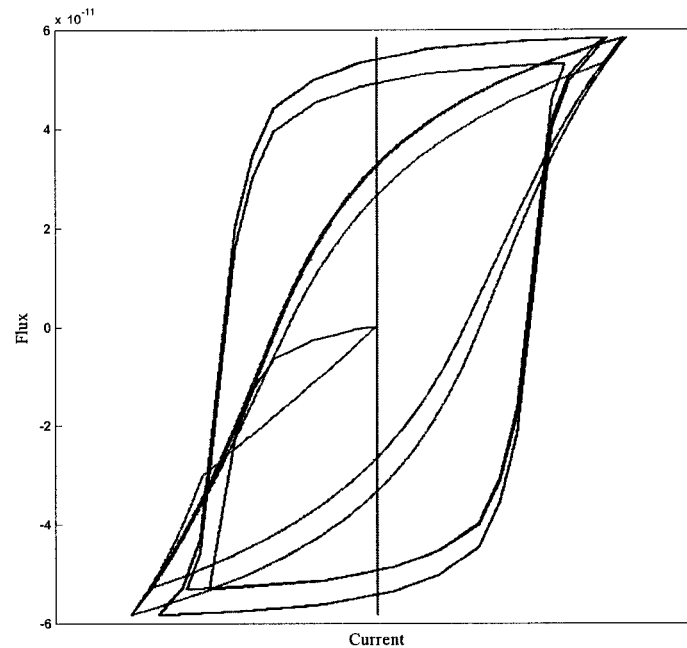
Figure 5-7   Effect of y_{rev} on the shape of minor loops: y_{rev} = 80% of maximum flux

The higher is the value of y_{rev} the thinner are the minor loops. It is normal to obtain such a result because of the second point on the minor loop (x_0, y_0) chosen to be at the origin, the reversal point (x_{rev}, y_{rev}) is not very far from the origin. Users can change manually this value to obtain better fitting of data.

The other parameters for minor loop modeling do not substantially modify the shape of minor loops. The default values can be chosen for most cases.

5.1.5 Fitting control parameters

The fitter uses a least-squares method for finding the saturation function parameters of equation (4.2). Three parameters control the convergence of this method:

- The convergence rate: Controls the convergence rate of the solution during optimization. Default is 10000.

- Maximum number of iterations: Maximum number of iterations in the fitting process. Default is 500.

- Convergence tolerance: Default is 0.1% of the smallest current value in the user-supplied flux-current characteristic.

5.1.6 A Numerical example

The characteristic of a 60 MVA power transformer has been used to present a numerical example for the hysteretic fitter. This is a 3-winding 24/6.8kV transformer. Its saturation characteristic is given in Figure 5-1 and minor loop data is shown in Figure 5-5. The fitter generates 2 files:

- A file containing hysteresis and saturation parameters defined by equations (4.2) and (4.9). It is possible to load this file into the hysteresis device data forms using the "Load data from file" option (see EMTPWorks). The extension of this file is .hys

- A file containing raw data and fitted data. The file extension is .fit. This file is used for verifying the fitting.

Figure 5-8 compares raw data corresponding to this transformer and fitted data. The requisite symmetry of the hyperbolic curves complicates the fitting if the available characteristic has a lack of symmetry. It also noticed that the fitting could have been improved if 3rd or 4th order equations were used instead of the quadratic model of equations (4.2) and (4.9).
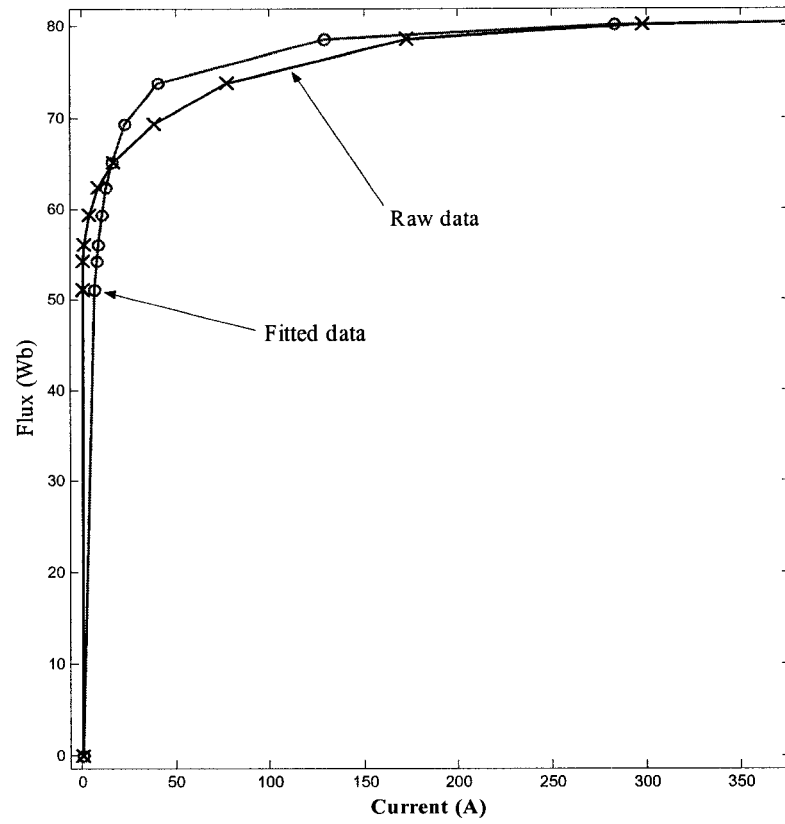
Figure 5-8   Fitting example

5.2 The hysteretic reactor

This section presents the implementation of the actual reactor model into EMTP-RV. To allow a completely general solution where nonlinear model functions can be solved without topological restrictions, EMTP-RV uses an iterative setup with the entire system of linear equations. Nonlinear devices are required to simply return their discretized Norton equivalent through linearization at the given operating point for time-point t. This modular and decoupled approach has been shown [15] to constitute a full Newton method.

5.2.1 Norton equivalent of the hysteretic reactor

As explained in [15] EMTP-RV requires both trapezoidal and Backward Euler numerical techniques implemented in all models. The Backward Euler method is used for eliminating numerical oscillations.

In EMTP-RV, the hysteretic reactor is a flux-input/current-output element. The relation between flux and current is given by:

$$\Phi_t = f(i_t) \tag{5.18}$$

with f a nonlinear function. At each solution time-point it is converted into the Norton equivalent shown in Figure 5-9.
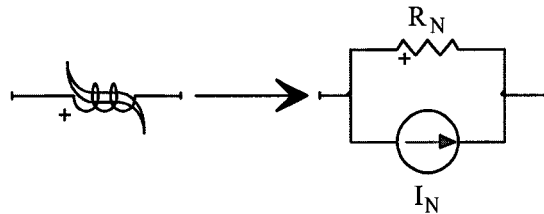

Figure 5-9   The hysteretic reactor and its equivalent circuit in EMTP-RV equations

The flux $\Phi_t^{(j)}$ (at time-point t and iteration j) is first found from the network voltage $v_t^{(j)}$:

$$\Phi_t^{(j)} = \int_{t-\Delta t}^{t} v_t^{(j)} dt + \Phi_{history_t} \qquad (5.19)$$

Using the trapezoidal integration method with time-step Δt we obtain the discretized version of the above equation:

$$\Phi_t^{(j)} = \frac{\Delta t}{2} v_t^{(j)} + \Phi_{history_t} \qquad (5.20)$$

This flux is entered into equation (4.2) as λ_{sat} to find λ_{unsat} and then into equation (4.9) to find the current on the undertaken trajectory and $\Phi_{q_t}^{(j)}$ (ordinate at the origin of the operating segment) in:

$$\Phi_t^{(j)} = K_{q_t}^{(j)} i_t + \Phi_{q_t}^{(j)} \qquad (5.21)$$

The calculation of $K_{q_t}^{(j)}$ requires the differentiation of both (4.2) and (4.9) :

$$K_{q_t}^{(j)} = \left. \frac{\partial \Phi}{\partial \lambda_{unsat}} \right|_{\Phi_t^{(j)}, \lambda_{unsat_t}^{(j)}} \left. \frac{\partial \lambda_{unsat}}{\partial i} \right|_{\lambda_{unsat_t}^{(j)}, i_t^{(j)}} \qquad (5.22)$$

It can be shown that the combination of (5.20) and (5.21) results into:

$$i_t = \frac{\Delta t}{2 K_{q_t}^{(j)}} v_t + \frac{1}{K_{q_t}^{(j)}} \left(\Phi_{history_t} - \Phi_{q_t}^{(j)} \right) \qquad (5.23)$$

It appears that:

$$R_N = \frac{2 K_{q_t}^{(j)}}{\Delta t} \qquad (5.24)$$

$$I_N = \frac{1}{K_{q_t}^{(j)}} \left(\Phi_{history_t} - \Phi_{q_t}^{(j)} \right) \qquad (5.25)$$

which corresponds to the circuit of Figure 5-9.

The history term related to the trapezoidal integration method is:

$$\Phi_{history_t} = \frac{\Delta t}{2} v_t + \Phi_{history_{t-\Delta t}} \qquad (5.26)$$

When Backward Euler rule of integration is used, the history becomes:

$$\Phi_{history_t} = \Phi_{history_{t-\Delta t}} \qquad (5.27)$$

The differential of the hysteresis curve (4.9) must be computed to find the Norton equivalent. But the function f is an implicit function composed of 2 quadratic

equations. That is why each equation (saturation and hysteresis) must be differentiated to find the final differential. The hysteresis equation gives the first differential:

$$\frac{\partial \lambda_{unsat}}{\partial i}\bigg|_{\lambda_{unsat_t},i_t} = \frac{b + a\,S_{hh}}{a + \dfrac{b}{S_{hv}}} \tag{5.28}$$

with :

$$a = i_t - \frac{\lambda_{unsat_t}}{S_{hv}} - X_{hv} \tag{5.29}$$

and :

$$b = i_t\,S_{hh} - \lambda_{unsat_t} + Y_{hh} \tag{5.30}$$

The saturation equation is based on equation (4.2), but a symmetry has been applied for negative flux and current. To compute the differential of this modified curve, both flux and current must be used with absolute values.

In its final form:

$$\frac{\partial \Phi}{\partial i}\bigg|_{\Phi_t,i_t} = \frac{(c + S_{sh}\,d)}{d + \dfrac{c}{S_{sv}}} \frac{\partial \lambda_{unsat}}{\partial i}\bigg|_{\lambda_{unsat_t},i_t} \tag{5.31}$$

with :

$$c = \lambda_{unsat_t}\,S_{sh} - \Phi_t + Y_{hh} \tag{5.32}$$

and:

$$d = \lambda_{unsat_t} - \frac{\Phi_t}{S_{sv}} - X_{sv} \tag{5.33}$$

The Norton equivalent is now known. This equivalent impedance network is the only the interface of the hysteretic reactor with the EMTP-RV computational engine.

5.2.2 Conformability to the "guess modification method"

The general theory of this method is presented in [15]. This section presents how the hysteretic reactor model equations have been made to account for this method. The "guess modification method" is designed to accelerate and in some cases provide local convergence for a nonlinear function. The modified guess for this device is the voltage, so it is a "voltage guess modification method".

In the iterative process at time-point t it is needed to compute the Norton admittance. To find $\dfrac{1}{R_N}$ it is needed to differentiate the hysteresis and saturation equations. Using the above $\dfrac{1}{R_N}$ in the linearization at operating point, gives:

$$I_t = I_N + \frac{v_t}{R_N} \tag{5.34}$$

The Norton equivalent circuit inserted into the main system of equations provides a new solution. This solution is on the straight line passing at the last operating point with the slope $\dfrac{1}{R_N}$. The difficulty with this approach is that in some cases it can result in numerical overflow conditions and/or an unnecessary large number of iterations [15]. Such a situation is illustrated in Figure 5-10 (the iteration count is k).
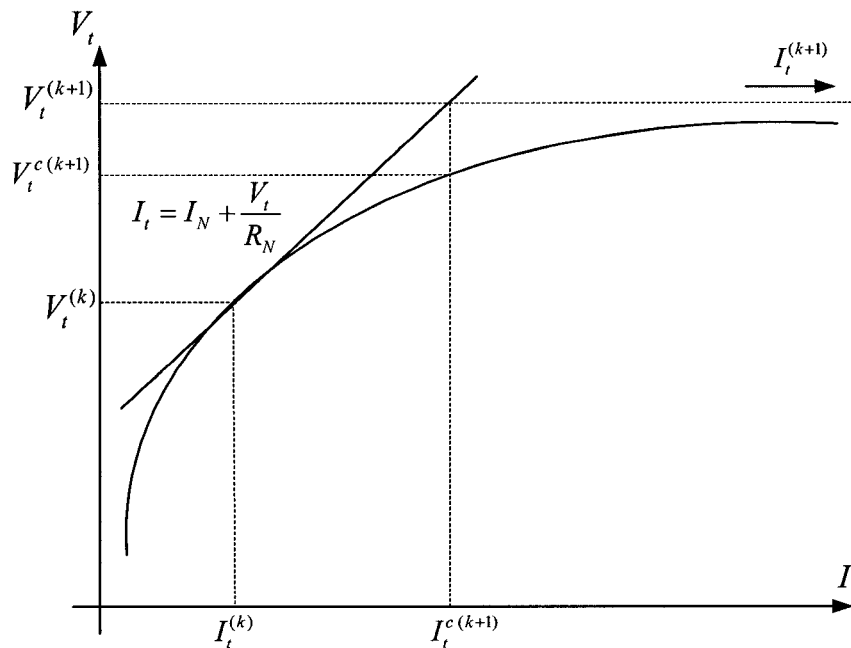

Figure 5-10   An example of the use of the Voltage guess modification method

The new hysteretic reactor voltage found from network conditions moves along the linearization at $v_t^{(k)}$ to give $v_t^{(k+1)}$. The current corresponding to this new voltage moves very far to the right on the saturation curve. This important excursion is not valid. To avoid such conditions, it is necessary to apply a correction to the voltage. It can be called a voltage guess modification or an adaptable Newton deceleration factor. It establishes a new operating point where linearization is again applied. To locate the corrected operating point, it is sufficient to find $v_t^{(k+1)}$:

$$I_N + \frac{v_t^{(k+1)}}{R_N} = I_t^{c\,(k+1)} \tag{5.35}$$

and to solve the nonlinear equation :

$$I_t^{c\,(k+1)} = f(\Phi_t^{c\,(k+1)}) \tag{5.36}$$

The function f is defined in equation (5.18). As a consequence f^{-1} must be found. Finding instantaneous flux from current is not easy because a reversal point can occur at the $k+1$ iteration count. In order to find which is the good branch to compute the voltage guess modification, it is assumed that the point found by first linearization (at iteration $k+1$) gives the good trajectory. Figure 5-11 explains this hypothesis.
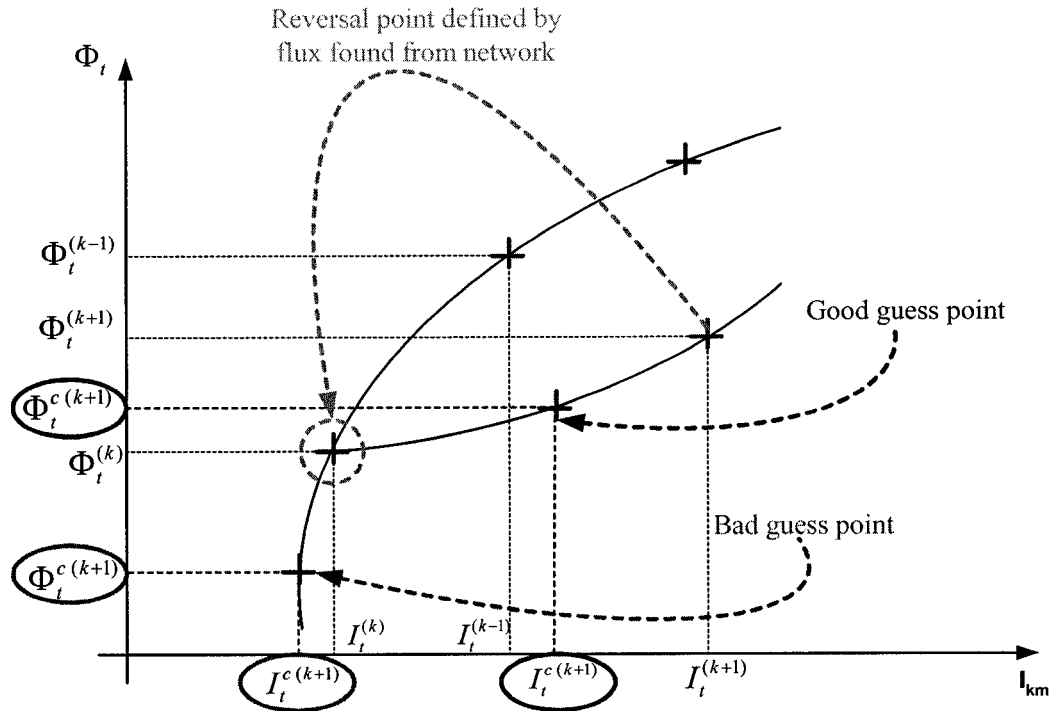
Figure 5-11   Choose good guess point for voltage guess modification method

It must be observed, however, that the voltage guess modification method can also result into an acceleration factor. Such a situation appears for downward trajectories. The corrected guess now goes further from the previous iteration flux than the guess provided by the standard method. This is why EMTP-RV always calculates guess point but selects it only if it is closer than $\Phi_t^{(k+1)}$ to $\Phi_t^{(k)}$.

5.2.3 Iteration panic method

In many cases nonlinear elements converge very quickly. In most topological conditions the hysteretic reactor converges in 2 or 3 iterations. In some cases a nonlinear device could have practically converged, but selected or default convergence tolerance is not reached. That is why before overtaking the maximum number of iterations (typically 300 iterations), EMTP-RV decreases the tolerance of convergence when the number of iterations exceeds a fixed number called iter_panic (default is 15 iterations). In this case the tolerance is multiplied by a factor (preset to 5). The iteration panic method is

particularly useful when a huge voltage change occurred, for instance, the energization of a transformer with hysteresis modeling.

6 Test Cases

6.1 First test case

This basic case provides a visual and theoretical validation. This case consists in opening a switch connected to a hysteretic reactor. When the switch opens current becomes zero and remanent flux is preserved. The simulated circuit is shown in Figure 6-1. Results are given in Figure 6-2, Figure 6-3, and Figure 6-4. The switch is closed at 1 ms and opened at 100 ms. Opening occurs on zero current.
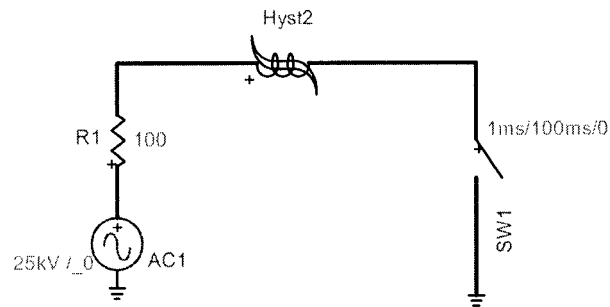
Figure 6-1   First test case circuit
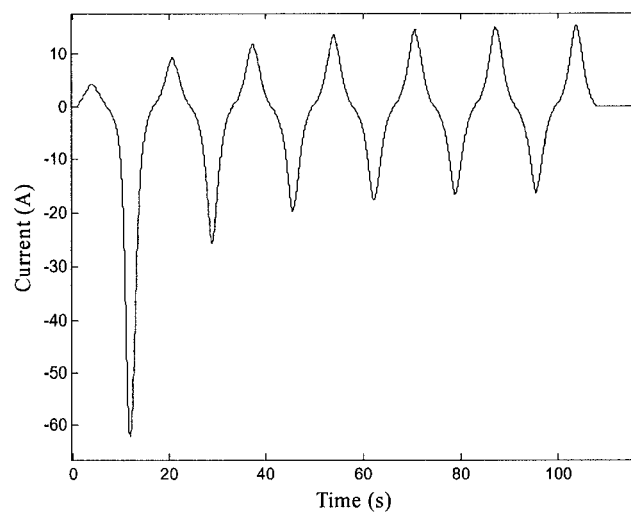
Figure 6-2   Inrush current in the hysteretic reactor of First test case

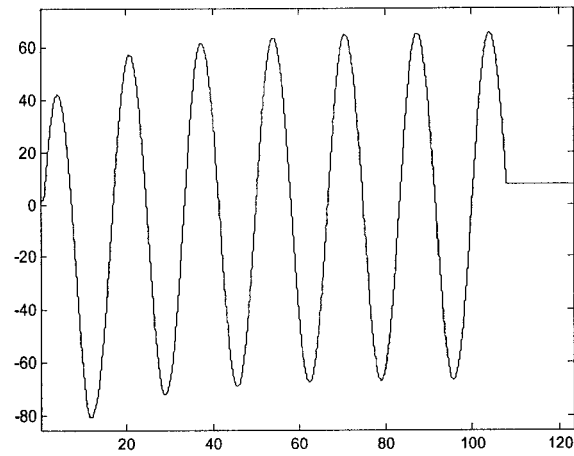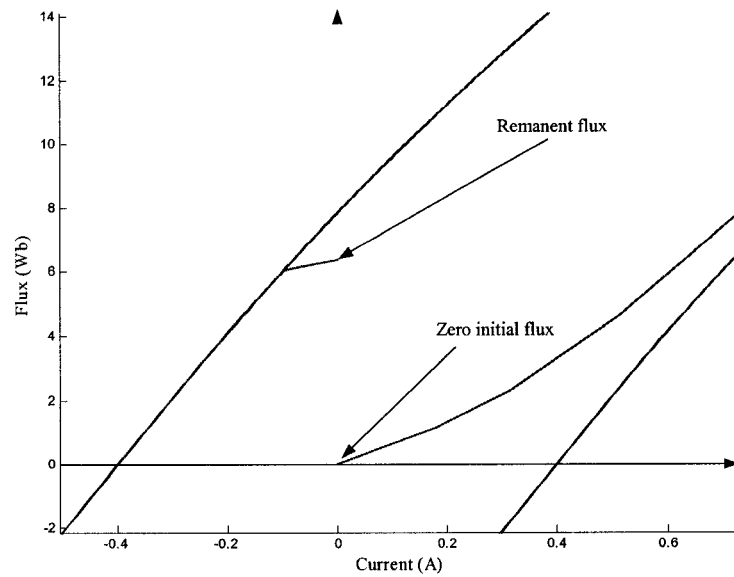**Figure 6-3   Flux in the hysteretic reactance of First test case**

Figure 6-4   Flux vs. current in the hysteretic reactor of First test case

The integration time step is $20\,\mu s$ and the simulation time is $200\,ms$. Relative convergence tolerance is 10^{-6}. Initial flux is zero, that is why first magnetizing curve starts at the origin. Zero initial conditions have been chosen.

The switch is opened when current is zero but the hysteretic reactor converges even if switch cuts a small current. Remanent flux takes place when the switch is opened at 40 ms (Figure 6-4). This case cannot be simulated with EMTP-V3 with any of available models.

6.2 A ferroresonance case, Second test case

Ferroresonance can occur in a distribution system where one or more of the supply conductors to an unloaded or very lightly loaded power transformer are interrupted or energized, leaving a transformer coil energized through the capacitive coupling with the others phases. In the distribution network, these situations are a single-pole circuit breaker opened by an operator, a single fuse blocking or a conductor rupture.

The ferroresonance problem, whether in a general circuit or in a power-system circuit, is usually tackled in one of two ways: circuit configuration (i.e. saturation and hysteresis of transformers). A fundamental factor to the occurrence of ferroresonance is the nonlinear magnetizing characteristic of the transformer and the capacitive coupling.

In order to reduce overvoltages caused by ferroresonance, MOVs (Metal Oxide Varistors) are installed. Two study questions must be answered: will the MOVs mitigate ferroresonance, and will the MOVs fail during ferroresonance.

Simulations for different operating conditions can be carried out in order to determine the maximum current and overvoltage. The modeling of the magnetization inductance in transformers is important in such cases: whether it can be modeled with nonlinear inductance or with hysteretic inductance. The hysteretic reactor introduces damping and gives more realistic overvoltages. In this part, the switching of a part of power-system circuit comprised of a cable connected to an unloaded transformer is carried out.

6.2.1 Configuration

In this case, a 250 kVA, 20/0.4 kV transformer is used. This transformer is represented by the hysteretic transformer model. A 100 m of cable with $R = 0.32\,\Omega/km$;

$L = 0.41 mH / km$; $C_1 = 0.22 \mu F / km$; $C_0 = 0.19 \mu F / km$ is used for this study. This cable is modeled by a π-section. The short-circuit power of the source is about 150 MVA.
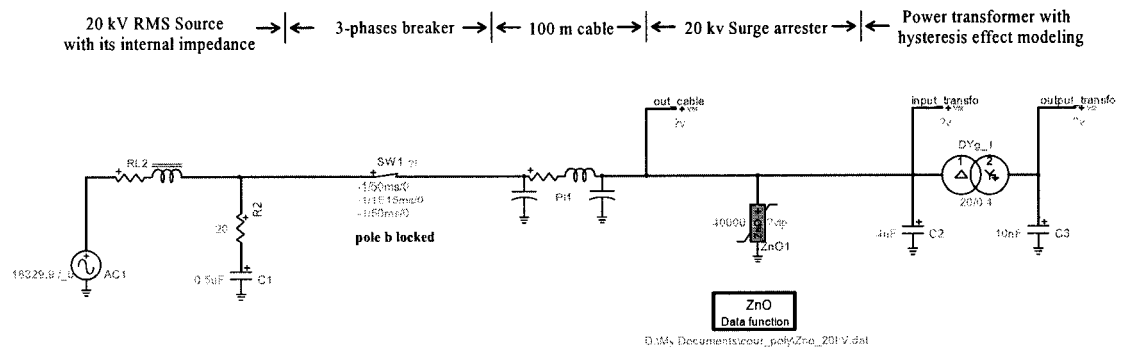
Figure 6-5   Simulation scheme generated is EMTPWorks for ferroresonance study

The configuration of the study is shown in Figure 6-5. The 3-phases power transformer is composed of 1-phase units including hysteretic reactances (see Figure 6-6). Fitting results are shown in Figure 6-7.
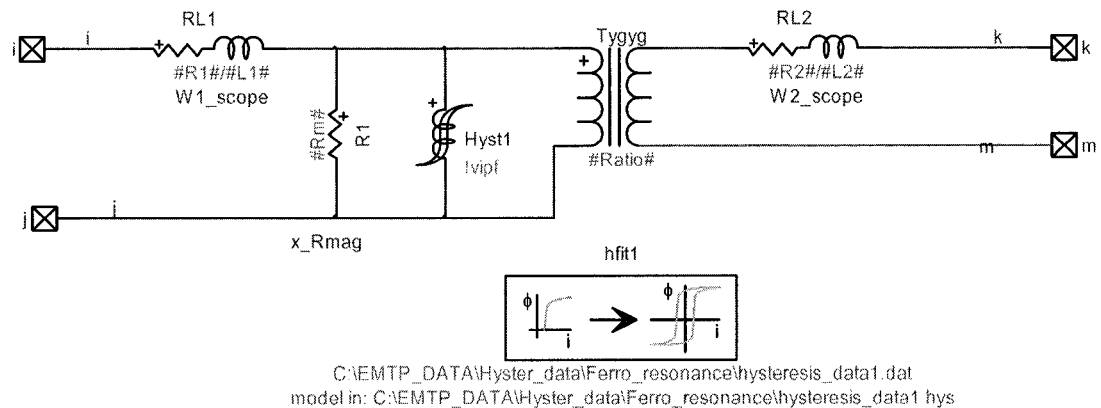
Figure 6-6   Internal model of each transformer phase including hysteretic effect
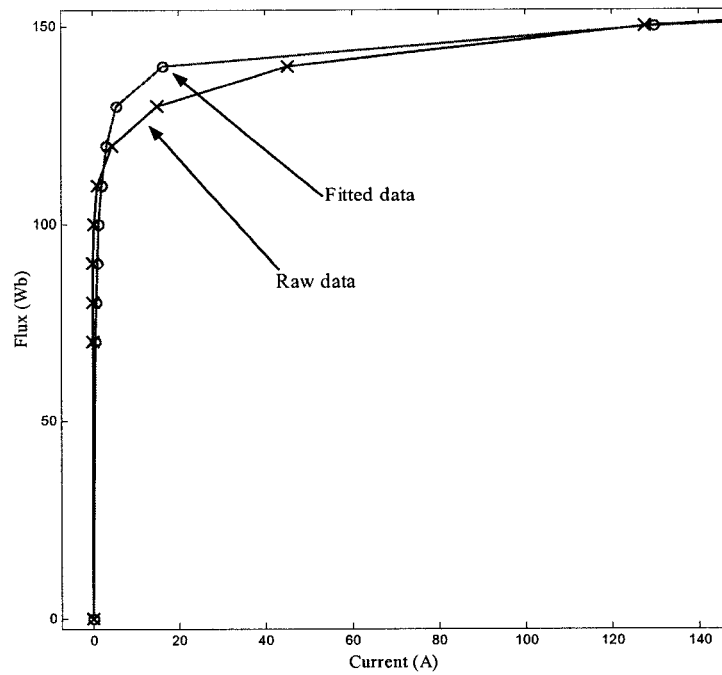
Figure 6-7   Hysteretic fitting results for the ferroresonance case

6.2.2 Simulation results

In this case, the switch on phase b stays closed while switches on phases a and c are opened at $t = 50\,ms$. The maximum overvoltage is 2.1 pu (4 pu without MOVs) as shown in Figure 6-8.
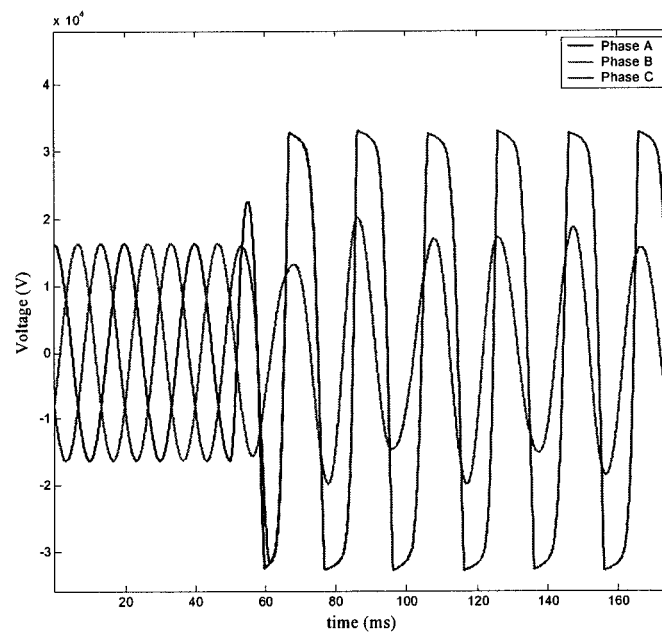
Figure 6-8   Voltage on primary of the transformer: ferroresonance waveforms
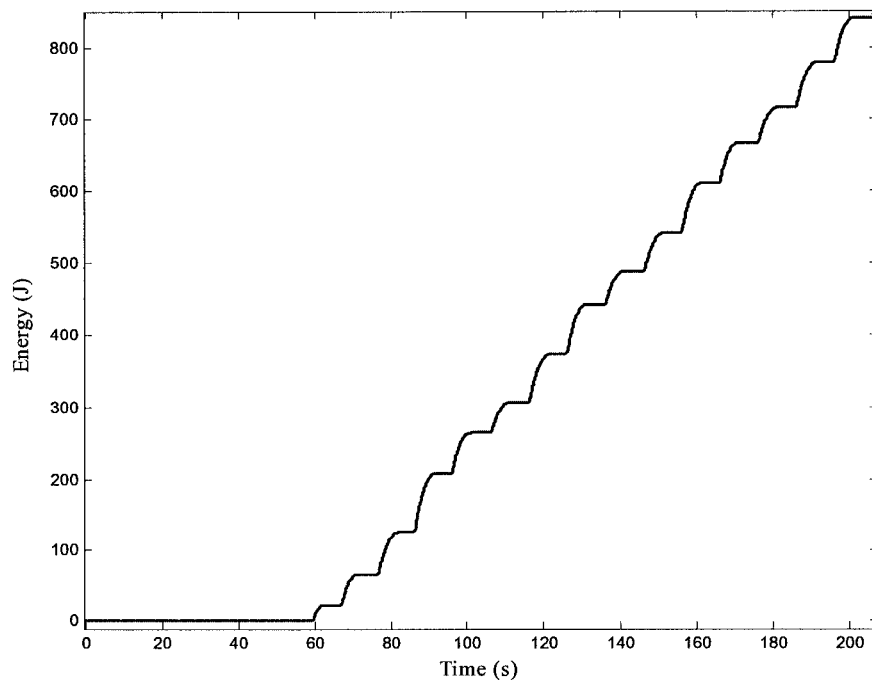
Figure 6-9   Absorbing energies of MOV

With the help of MOVs, overvoltages can be reduced. Figure 6-9 shows that if absorbing energies of MOVs are superior to their limits, MOVs can fail during ferroresonance.

An other ferroresonance test case is also explained in Appendix A : Ferroresonance Test Case.

6.3 A practical test case taken from the EDF system, Third test case

This case is taken from [17]. This publication is given in Appendix B : Paper for IPST 2003 Conference. Its data is taken from an EDF (Électricité de France) system configuration.

6.3.1 Configuration

A high-level view of the selected test case is shown in Figure 6-10. The test case studies the energization of a set of two interconnected target transformers (three-pole 3x360 MVA and three-phase 2x29 MVA) when a second 600 MVA transformer has been already energized through a long line. The generator at the sending end is a 900 MW machine, which is modeled as an ideal source behind its subtransient reactance. The long line and the interconnecting cables are modeled using pi-sections. The detailed case includes a total of 5 transformers: an autotransformer at the receiving end of the line, the step-up transformer at the source end, the load transformer at the source end, the step-down target transformer and the second load transformer at the target. The target transformers are modeled using the hysteretic reactor model presented in this paper. This approach allows to account for remanent flux at energization. All other transformers contain a nonlinear inductance. All nonlinear models are solved simultaneously with the linear network using the techniques available in EMTP-RV. The programming of the hysteretic reactor contributed in this work.
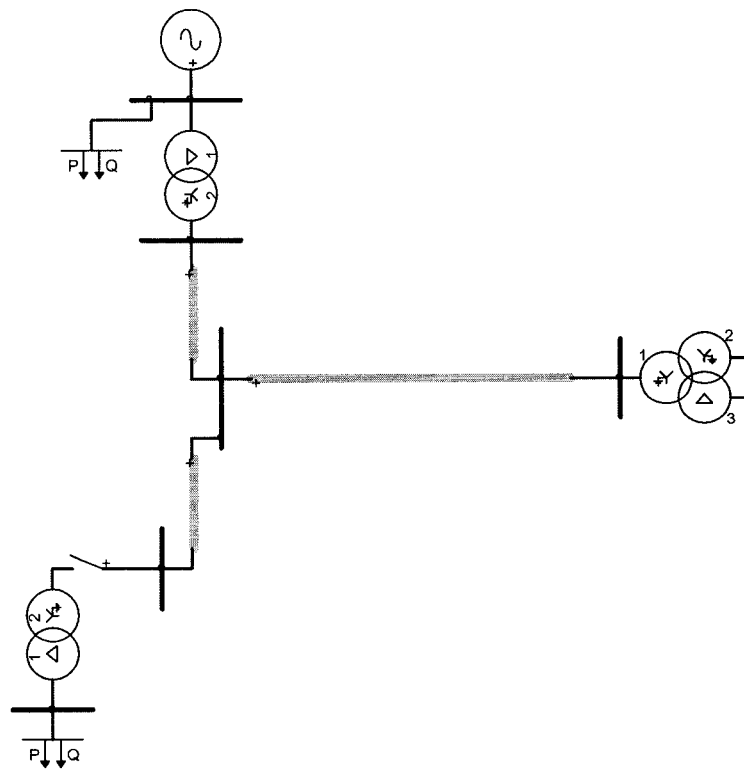
Figure 6-10   Simulated case from EDF network

This case as assembled could not be solved using previously available EMTP-V3 methods [3]. In addition to the fact that the previously programmed compensation technique did not allow mixed nonlinear functions, both the Type-92 and Type-96 hysteretic models were unable to achieve convergence.

6.3.2 Simulation results

The breaker shown in Figure 6-10 is initially closed to establish steady-state conditions. It is then opened at 10 ms and reclosed again at 1.7 s. Figure 6-11 shows the phase-a voltage at the breaker. The red line (solid line) is using the hysteretic reactor model, while the blue (dotted line) shows the same simulation when a simple nonlinear inductance is used to model saturation. It is apparent that due to its ability to maintain

remanent flux, the hysteretic reactor is allowing to observe an overvoltage of approximately 1.7 pu.
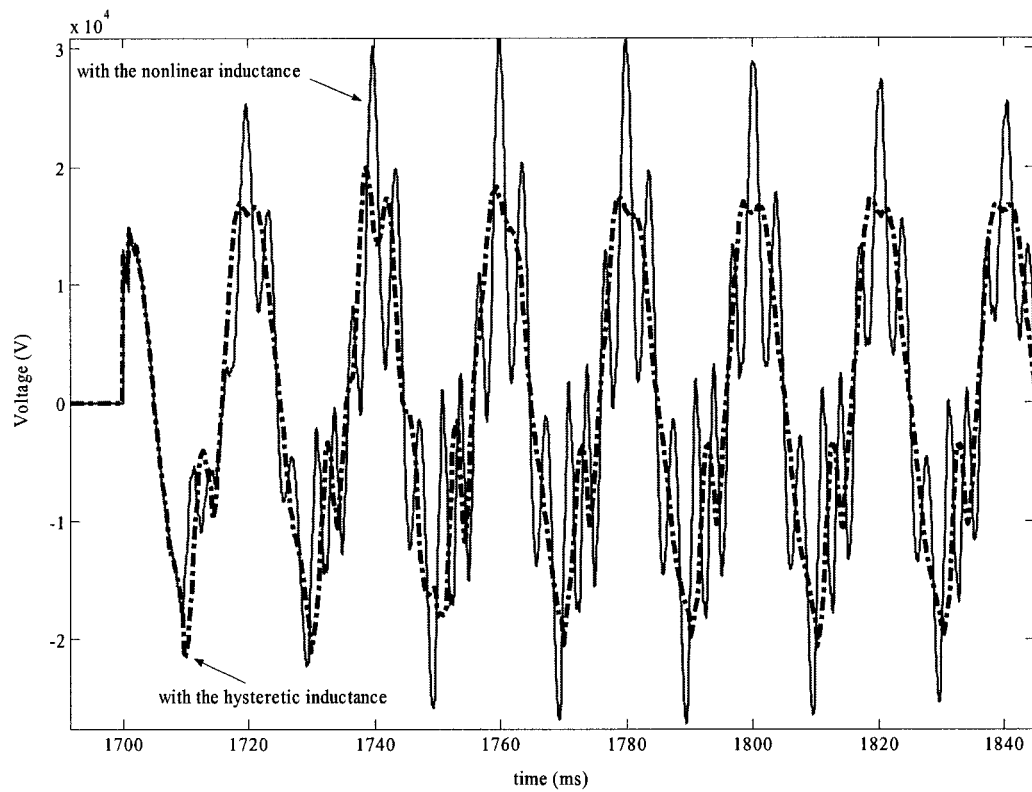
Figure 6-11   Energization of target transformers, phase-a voltage at the breaker

Figure 6-12 presents a view of hysteresis trajectories for phase-a of the first target transformer. The reactor is on a steady-state trajectory before the occurrence of the transient that moves on the minor loops.
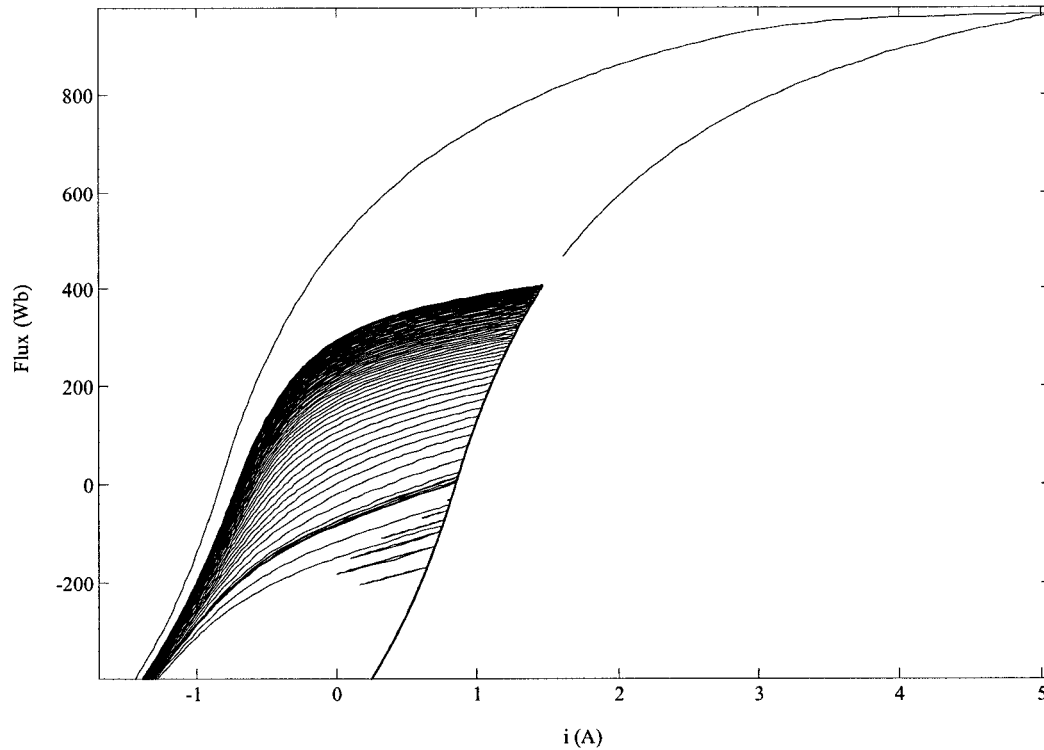
Figure 6-12 Hysteresis trajectories for phase-a of reenergized target transformer

It is valuable to mention that the mean number of iterations per time-point is about 2.21 and the total CPU time is 60 s for a simulation interval of 3 s using $\Delta t = 50 \mu s$ on a Pentium-4 computer of 1.7 GHz. The complete network contains a total of 200 nodes and 250 devices. The simulation time is dramatically reduced by the ability of the setup to achieve steady-state conditions at simulation startup.

7 Conclusions

This work has presented the implementation of a new hysteretic reactor model for transient analysis. The model has been demonstrated using the EMTP-RV environment. The physical model as such, has been derived from previously available work, but its numerical solution and implementation are new. Several not previously explained aspects of the model have been also presented.

Important problems, such as initialization, fitting and integration into a Newton solution have been solved. The main advantages of this model as compared to previously available models in EMTP can be briefly summarized as follows:

- This model has the inherent ability to achieve a simultaneous solution with network equations in arbitrary and unrestricted topological configurations. EMTP-RV uses an iterative setup with the entire linear equations to constitute a Newton method. This approach has a significant impact on the probability of convergence of the model for a given integration time-step.

- The hysteresis fitting method has been improved to decrease the difference between raw and fitted data. A large number of control techniques have been applied at each step of the fitting process to assess the validity of results.

- The model is efficient and does not appreciably increase the computer time for large scale networks when replacing the simple nonlinear inductance model.

The model has been used in practical test cases of transformer energization. The test case solutions have achieved new and not previously available simulation capabilities.

Improvements of the present work can be done in using 3rd or 4th order equations instead of quadratic equations for the hysteresis model. The requisite symmetry of the hyperbolic curves complicates the fitting if the available characteristic has a lack of symmetry. Another area in which it will probably be possible to extend this work is in the modeling of frequency dependant hysteresis effect.

The programming of the model in the official version of EMTP-RV makes it of industrial grade: user-friendly, efficient and reliable. The actual code is object-oriented, applies modularity and encapsulation and is fully documented. The work presented in this document can be easily extended to include future improvements and to support research activities in this field.

References

[1] J. Mahseredjian, L. Dubé, L. Gérin-Lajoie, "New advances in the Simulation of Transients with EMTP: Computation and Visualization Techniques", Electrimacs, August 19th, 2002, Plenary session paper.

[2] J. Mahseredjian, "EMTPWorks, a graphical user interface for EMTP", Hydro-Québec, 2002

[3] Electromagnetic Transients Program (EMTP), EMTP-V3 Rule Book I, Development Coordination Group of EMTP, 1996.

[4] A. Narang, E. P. Dick, R. C. Cheung "Transformer Model for ElectroMagnetic Transient Studies", CEA Report 175 T 331 G, December 1996.

[5] E. P. Dick and W. Watson, "Transformer Models for Transient Studies Based on field Measurements", IEEE Transactions on Power Apparatus and Systems, Vol. PAS-100, No. 1, January 1981, pp. 409-419.

[6] D. C. Jiles and D. L. Atherton, "Ferromagnetic hysteresis" IEEE, Transaction Magn, vol. MAG-19, pp 2183-2185, Sept. 1983.

[7] S. R. Naidu, ME, PhD, "Simulation of the hysteresis phenomenon using Preisach's Theory" IEE Proceedings, Vol. 137, Pt. A, No. 2, March 1990.

[8] Glenn W. Swift, "Power transformer Core Behavior Under Transient Conditions" IEEE Transactions PAS, September/October 1971, pp2206-2210.

[9] J. G. Frame, N. Mohan, T Liu, "Hysteresis Modeling in an Electromagnetic Transients Program", IEEE Trans. Vol PAS-101, No. 9, Sept 1982 pp 3403-3412.

[10] S. N. Talukdar and J. R. Bailey, "Hysteresis Model for System Studies" IEEE Trans. on PA&S, PAS-95, pp1429-1434, July/August 1976.

[11] D. N. Ewart, "Digital Computer Simulation Model of a Steel-Core Transformer", IEEE Transactions on Power Delivery, July 1986.

[12] H. W. Dommel: "Nonlinear and time-varying elements in digital simulation of electromagnetic transients". IEEE Transactions, PAS, Vol. 90, pp. 2561-3567, 1971

[13] J. Mahseredjian, S. Lefebvre and X.-D. Do: "A new method for time-domain modelling of nonlinear circuits in large linear networks". 11th Power Systems Computation conference (PSCC), Proceedings Vol. 2, August 1993, pp. 915-922

[14] Electromagnetic Transients Program (EMTP), EMTP-V3, Rule Book II, "Fitsat" auxiliary function.

[15] J. Mahseredjian, "EMTP-RV : The design of Version 0A" Third report for CEA contract NO. C980700-9998 (EMTP Restructuring Project), January 2000.

[16] A. Semlyen and A. Castro, "A digital Transformer Model for switching transient calculations in three phase systems", PICA Conf, 9th, Proc, New Orleans, LA, June 2-4, 1975, p. 121-126.

[17] S. Dennetière, J. Mahseredjian, "On the Implementation of a hysteretic reactor model in EMTP", paper accepted for IPST 2003 Hong-Kong Conference

[18] Jacobson D.A.N., Marti, L., Menzies, R.W., "Modeling Ferroresonance in a 230 kV Transformer-Terminated-Double-Circuit Transmission Line", Processings of the IPST 1999 Budapest Conference, pp. 451-456, June 20-24

Appendix A : Ferroresonance Test Case

A possible ferroresonant circuit condition occurs when an unloaded transformer is connected to a de-energized transmission line that is capacitively coupled with a parallel energized line. An example from Manitoba Hydro's 230 kV power system is investigated through EMTP simulations and field tests in Reference [18]. This case was provided by Jacobson D.A.N. from Manitoba Hydro. Naoual Rar, a graduate student from the École Polytechnique de Montreal, has contributed the creation and the simulation of this case in the EMTPWorks environment.

The transformer model (including hysteresis effect) is known to greatly influence the ferroresonant state. That is why, such an example is a good validation test for the hysteresis model presented in this work. The results given by EMTP-RV were compared with EMTP-V3 results and fields tests presented in [18]. However it is noticed that it was a much difficult setup requiring several extra manipulation setups until desired results were achieved. The overall results remain less accurate due to problems for solving nonlinear functions.

A diagram representing the studied system is given in Figure 7-1. The literature indicates ferroresonance will be excited only for a narrow band of initial conditions. Hence, the probability is low even if the configuration is of high risk. Figure 7-2 shows that the new hysteresis model is reliable enough to represent ferroresonance. Frequency analysis of resulting signals also validated the new model. Field measurements show that the ferroresonant waveforms have a 25 Hz fundamental frequency. Figure 7-3 is a Fourier Transformation of ferroresonant waveform voltage on phase a of the arrester. The magnitude of the voltage has a peak value near 25 Hz. As a consequence the new hysteresis model is also validated by frequency analysis.

Figure 7-1   Circuit model of the Manitoba Hydro test case

Figure 7-2   Ferroresonance of transformer with the coupled line, phase-a voltage at the arrester
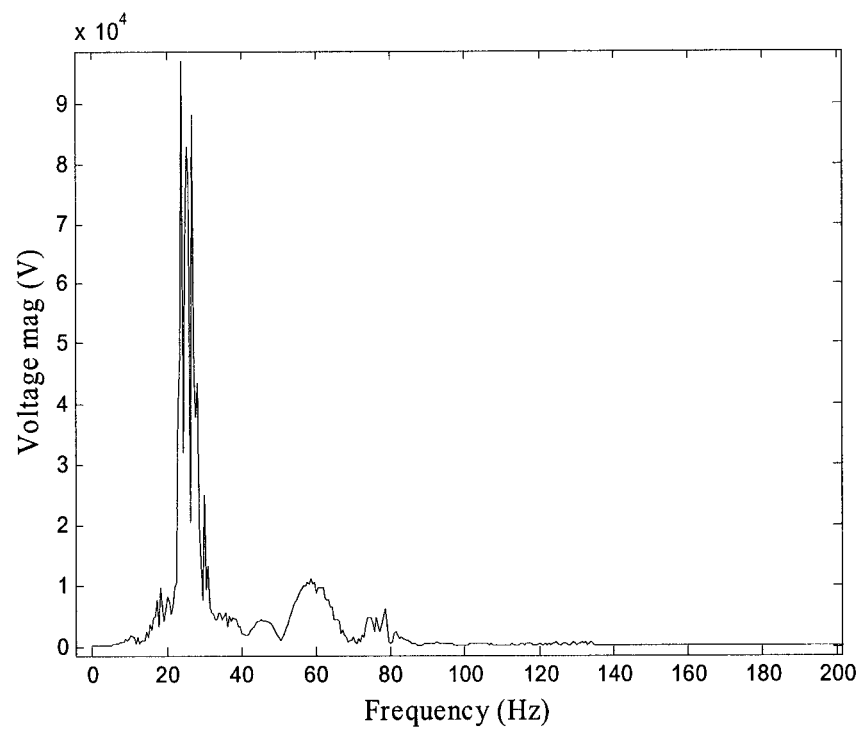
Figure 7-3 **Frequency analysis of ferroresonant waveform voltage, on phase a of the arrester**

Appendix B : Paper for IPST 2003 Conference

On the implementation of a hysteretic reactor model in EMTP

Sébastien Dennetière[1], Jean Mahseredjian[1], Manuel Martinez[2], Michel Rioual[2], Alain Xémard[2],
Patrick Bastard[3]

(1)IREQ / Hydro-Québec	(2)Électricité de France	(3)Supélec
1800 Lionel-Boulet	Direction des Études et	Plateau de Moulon – 3 Rue
Varennes, Québec,	Recherches	Joliot-Curie
Canada, J3X 1S1	1 ave. du Général de Gaulle	91190 Gif-sur-Yvette
	92141 Clamart Cedex	Cédex, France

Abstract - This paper presents the implementation of a hysteretic reactor model in a transient analysis package. The model is available in a currently developed EMTP (DCG-EPRI) version. It is demonstrated how the hysteretic reactor equations can be solved to eliminate topological limitations and allow solving large scale networks efficiently. Numerical robustness aspects and the representation of minor loops are emphasized. The model demonstrates new and not previously available computational capabilities.

Keywords: Hysteresis, transients, nonlinearities, EMTP

I. INTRODUCTION

Magnetic hysteresis plays an important role in certain analysis cases associated with power systems. Practical examples are the inrush current and ferroresonance. The inclusion of a hysteresis branch in a transformer model allows representing residual flux effects and provides increased accuracy in the computation of losses. The challenge of an EMTP type model is to correctly simulate hysteresis with the inherent complexities related to minor loops.

The most commonly used hysteretic reactor model in EMTP is the pseudononlinear Type-96 model [1]. The pseudononlinear term implicates that the reactor is not solved simultaneously with the surrounding network equations. In addition to the well known limitations of such an approach, the Type-96 modeling assumptions make it a poorer candidate for matching experimental results.

In addition to this model, EMTP has recently introduced the Type-92 model [2]. This model is classified as a true-nonlinear model and therefore has the inherent ability to achieve a simultaneous solution with network equations. It remained however prone to numerical problems and limitations mainly due to the applied solution method for true-nonlinear models. Other aspects,

such as the data fitting procedure, were using a less accurate method.

This paper starts by a summarized presentation on the limitations of the previously available EMTP models. It follows by the presentation of a new solution method for a physical model derived from [2][3]. Other details on the actual model are also provided.

The new implementation demonstrates unsurpassed capability for the simulation of large scale networks with hysteretic reactors located in arbitrary network configurations. A practical test case taken from the EDF (Electricité de France) system is shown to attain good numerical accuracy without degrading simulation performance.

II. PREVIOUS MODELS

The original EMTP Type-96 model is based on the theory developed in [4]. The hysteresis loops are modeled with piecewise linear approximations. Downward and upward trajectories are related by a translation on the x-axis and the minor loops are scaled in shape from the major loops. Some modifications have been proposed [5] to match experimental results. The model remained however unable to reproduce the experimental results presented in [3].

The minor loops trajectories of the Type-96 model were defined in terms of the major loop. In reality the minor loops have been shown to behave independently from the major loop trajectories. The Type-96 also assumed a single-valued characteristic for high currents.

In addition to physical modeling assumptions the Type-96 implementation was based only on the pseudo-nonlinear solution method of EMTP. This method converts the hysteresis slopes into a Norton equivalent which represents the relation between voltage and current at the given operating point and simulation time. Since there are no iterations it cannot be qualified as a simultaneous solution. The program changes operating segments only after illegally operating outside the range of the previous segment for one

time-step. This results into the typical noisy behavior shown in Figure 1. The integration time-step can be reduced to minimize such problems, but its drawback is a dramatically increased simulation time.
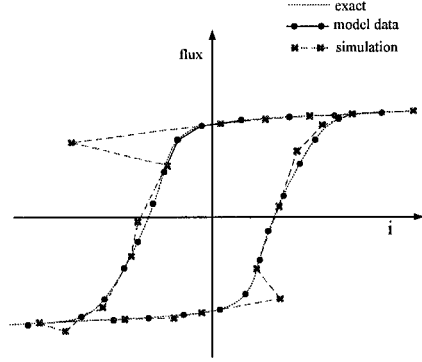

Figure 1 A test case with the Type-96 model

The Type-92 model was based on the flux distortion view of saturation [3][6]. It has been programmed using the true-nonlinear compensation method [7] based solution technique of EMTP. This method can provide a simultaneous solution with network equations but imposes several significant topological and numerical limitations described in [8]. Among such limitations are the inability to include the hysteresis model with other nonlinear models in the same subnetwork and matrix singularity conditions.

III. THE NEW MODEL

The hysteresis concept used by the new model is identical to the one proposed in [6]. The minor hysteresis loops are modeled using templates [3]. Each minor loop curve returns to the last reversal point from the current reversal point. The minor loops are closed upon exit and the trajectory is reverted back to the previous encompassing loop.

A. Modeling equations

Two separate functions are used. The first function is a hysteresis function relating 'unsaturated' flux λ_{unsat} to current. This function models the pure hysteresis effect. The second function is a saturation function relating instantaneous 'saturated flux' λ_{sat} to 'unsaturated' flux λ_{unsat}. This function represents the saturation effect. Both functions are geometrically represented by hyperbolic equations [2][9].

The saturation effect is given by:

$$C_{sat} = \left[\lambda_{unsat} - \frac{\lambda_{sat}}{S_{sv}} - X_{sv}\right]\left[S_{sh}\lambda_{unsat} - \lambda_{sat} + Y_{sh}\right]$$

(1)

The constant C_{sat} defines the curvature, it controls how close the curve is to its asymptotes. S_{sv} is the slope of the vertical asymptote, S_{sh} is the slope of the horizontal asymptote, X_{sv} is the x-axis intercept of the vertical asymptote and Y_{sh} is the y-axis intercept of the horizontal asymptote. Once the main shape of the saturation curve is defined, the concave function part is taken for positive values of λ_{unsat} and λ_{sat}. The relation between negative values is obtained by symmetry. The final saturation curve passes through the origin.

The relation between λ_{unsat} and current i is given by:

$$C_{hyst} = \left[i - \frac{\lambda_{unsat}}{S_{hv}} - X_{hv}\right]\left[S_{hh}i - \lambda_{unsat} - Y_{hh}\right]$$

(2)

The C_{hyst} defines the hysteresis effect curvature. The remaining variables are defined as in equation (1), but for the hysteresis effect. In this case the convex branch is chosen for the upward trajectory and the concave branch for the downward trajectory. Since it is needed to establish a closed shape, a movement of translation is performed on the asymptotes. Figure 2 shows the initial curve (solid blue line) and the translated curve (red dashed line). The curves 1 and 2 form the hysteresis loop.
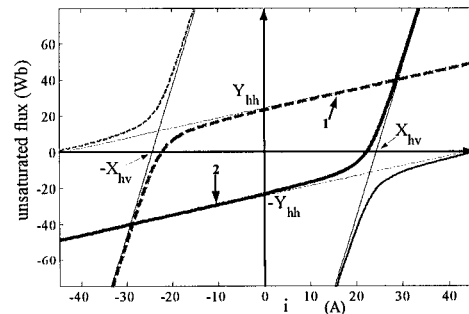

Figure 2 Hysteresis modeling template

B. Hysteresis trajectories

Hysteresis trajectories follow a uniform template. Upward and downward trajectories correspond to opposite template orientations. The

parameters X_{hv} and Y_{hh} control template position and are systematically modified during simulation. The parameters C_{hyst}, S_{hv} and S_{hh} are fixed and define template shape. Since template shape is independent of its position, the starting point for a trajectory (reversal point on the hysteresis loop) is chosen as the origin of the coordinate system. Then in accordance with the model, the vertical asymptote (slope S_{hv}) is displaced to the right (or to the left for downward trajectory) along the abscissa by a distance equal to twice the coercive current. A minor loop trajectory cannot exceed the major loop asymptote.

When a reversal point is detected, a new trajectory begins. A reversal point occurs when the flux $\phi(t+\Delta t) < \phi(t)$ on an upward trajectory or when $\phi(t+\Delta t) > \phi(t)$ on a downward trajectory. The reversal points preceding the current loop must be saved. Hyperbolic branches automatically pass through the previous to last reversal point. Figure 3 illustrates the progression from the inner loop A. When the flux increases beyond the reversal point 5, the reversal point that defines the trajectory is 4. That is why a reversal point stack composed of (λ_{unsat}, i) value pairs is used to save the reversal points out of the present loop.
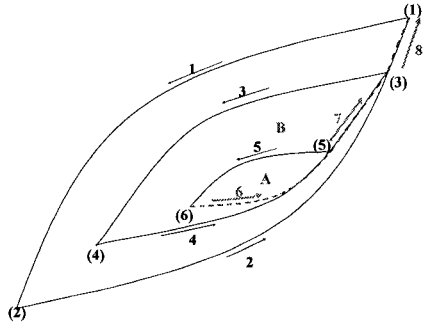

Figure 3 Reversal points in hysteresis trajectories

C. Initialization

Before starting the time loop solution, it is needed to initialize the reversal points stack. The first 2 points of this stack are initialized with very high flux (10^{10} Wb) for defining the borders of the major loop. The remaining variables depend on the type of initialization.

If 'manual' initial conditions (manual remanent flux ϕ_0) are used then the initialization proceeds as shown in Figure 4. Point 2 (current i_2) is arbitrarily chosen for a

current 50 times the coercive current. The next step is to determine equation (2) for a trajectory passing through ϕ_0 which will give point 1. It is assumed that the trajectory between the last reversal point and ϕ_0 is a downward trajectory if $\phi_0 \geq 0$ and upward trajectory if $\phi_0 < 0$. Such behavior is consistent with the deenergization pattern of a transformer. The point 2 is chosen sufficiently high to enable placing ϕ_0 on the upper trajectory between 2 and 1 when $\phi_0 \geq 0$ and on the lower trajectory when $\phi_0 < 0$. If this condition is not satisfied then point 2 must be moved. The same technique is applicable to $\phi_0 = 0$.
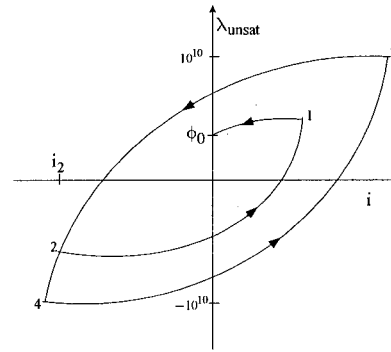

Figure 4 Reversal points stack for manual initial conditions

If it is chosen to connect the reactor during the steady-state phasor solution, one option is to use an inductance value taken from the slope of the major hysteresis loop at zero flux. In this case the initialization points are given in Figure 5. Points 3 and 4 are defined using $10\phi_{ss}$. The choice of $10\phi_{ss}$ (where ϕ_{ss} is the flux at t=0 from the steady-state phasor solution) is again arbitrary, but has been found acceptable in most cases.
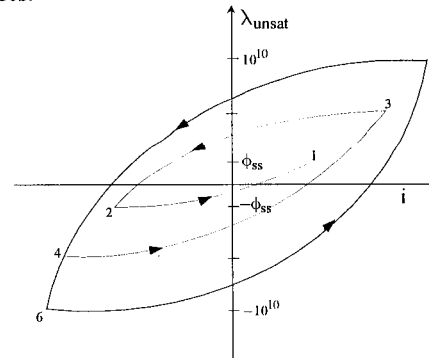

Figure 5 Reversal points stack initialization from steady-state

IV. IMPLEMENTATION IN EMTP

A. The fitter

As a first step it is required to provide a fitting method for determining the parameters of equations (1) and (2). The new fitter uses a least-squares method for finding the saturation function parameters of equation (1). The parameter S_{hv} of equation (2) is also determined by this method since during the fitting process λ_{unsat} is replaced by $S_{hv}i$. The remaining parameters of equation (2) are determined from minor loop data. The coercive current is determined from the major loop data or can be entered manually when only a centered raw data is available. The user is allowed to visualize the fitting results and improve them by manipulating parameters.

Figure 6 compares a case of raw data with fitted data. The requisite symmetry of the hyperbolic curves complicates the fitting if the available characteristic has a lack of symmetry. It also noticed that the fitting could have been improved if 3rd or 4th order equations were used instead of the quadratic model of equation (1).
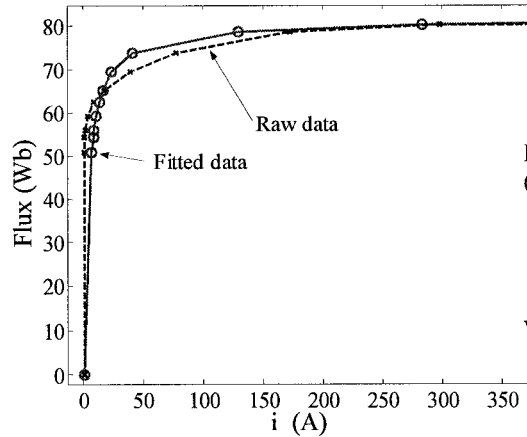

Figure 6 Fitting example

B. Equivalent circuit

The new hysteretic reactor has been implemented into a new EMTP code, named EMTP-RV [10][11]. To allow a completely general solution where nonlinear model functions can be solved without topological restrictions, EMTP-RV uses an iterative setup with the entire system of linear equations. Nonlinear devices are required to simply return their discretized Norton equivalent through linearization at the given operating point for time-point t. This constitutes a Newton method.

In EMTP-RV, the hysteretic reactor is a flux-input/current-output element. At each solution time-point it is converted into the Norton equivalent shown in Figure 7. This is similar to the nonlinear inductance model. The flux $\phi_t^{(j)}$ (at time-point t and iteration j) is first found from the network voltage $v_t^{(j)}$ using the trapezoidal integration method with time-step Δt:

$$\phi_t^{(j)} = \frac{\Delta t}{2} v_t^{(j)} + \phi_{history}$$

(3)

This flux is entered into equation (1) as λ_{sat} to find λ_{unsat} and then into equation (2) to find the current on the undertaken trajectory and $\phi_{q_t}^{(j)}$ (ordinate at the origin of the operating segment) in:

$$\phi_t^{(j)} = K_{q_t}^{(j)} i_t + \phi_{q_t}^{(j)}$$

(4)

The calculation of $K_{q_t}^{(j)}$ requires the differentiation of both (1) and (2):

$$K_{q_t}^{(j)} = \left. \frac{\partial \phi}{\partial \lambda_{unsat}} \right|_{\phi_t^{(j)}, \lambda_{unsat_t}^{(j)}} \left. \frac{\partial \lambda_{unsat}}{\partial i} \right|_{\lambda_{unsat_t}^{(j)}, i_t^{(j)}}$$

(5)

It can be shown that the combination of (3) and (4) results into:

$$i_t = \frac{\Delta t}{2 K_{q_t}^{(j)}} v_t + \frac{1}{K_{q_t}^{(j)}} \left(\phi_{history} - \phi_{q_t}^{(j)} \right)$$

(6)
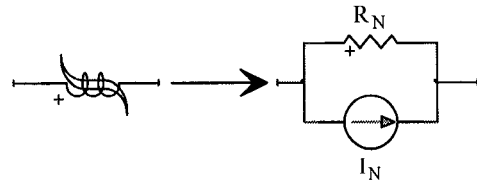
which corresponds to the circuit of Figure 7.

Figure 7 Hysteretic reactor equivalent circuit

This new approach has a fast convergence attribute by achieving the best available prediction for next time-point due to the linear solution movement with the nonlinear function of the reactor.

V. TEST CASE

A high-level view of the selected test case is shown in Figure 8. The test case studies the energization of a set of two interconnected target transformers (three-pole 3x360 MVA and three-phase 2x29 MVA) when a second 600 MVA transformer has been already energized through a long line. The generator at the sending end is a 900 MW machine, which is modeled as an ideal source behind its subtransient reactance. The long line and the interconnecting cables are modeled using pi-sections. The detailed case includes a total of 5 transformers: an autotransformer at the receiving end of the line, the step-up transformer at the source end, the load transformer at the source end, the step-down target transformer and the second load transformer at the target. The target transformers are modeled using the hysteretic reactor model presented in this paper. This approach allows to account for remanent flux at energization. All other transformers contain a nonlinear inductance. All nonlinear models are solved simultaneously with the linear network using the techniques developed in EMTP-RV [10].
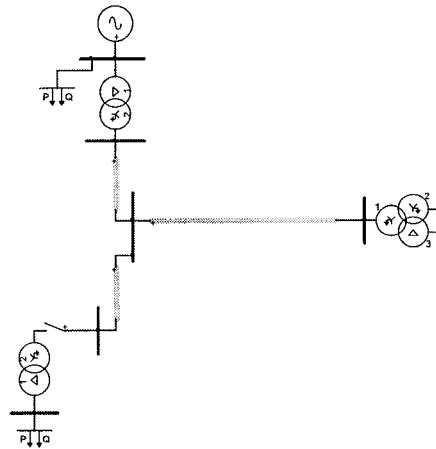

Figure 8 Simulated case

This case as assembled, could not be solved using previously available EMTP methods [1]. In addition to the fact that the previously programmed compensation technique did not allow mixed nonlinear functions, both the type-92 and type-96 hysteretic models were unable to achieve convergence.

The breaker shown in Figure 8 is initially closed to establish steady-state conditions. It is then opened at 10 ms and reclosed again at 1.7 s. Figure 9 shows the phase-a voltage at the breaker. The red line (solid line) is using the hysteretic reactor model, while the blue (dotted

line) shows the same simulation when a simple nonlinear inductance is used to model saturation. It is apparent that due to its ability to maintain remanent flux, the hysteretic reactor is allowing to observe an overvoltage of approximately 1.7 pu.
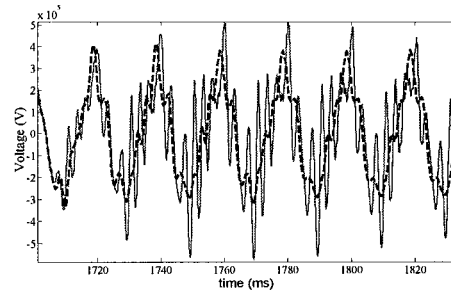

Figure 9 Energization of target transformers, phase-a voltage at the breaker

Figure 10 presents a view of hysteresis trajectories for phase-a of the first target transformer. The reactor is on a steady-state trajectory before the occurrence of the transient that moves on the minor loops.
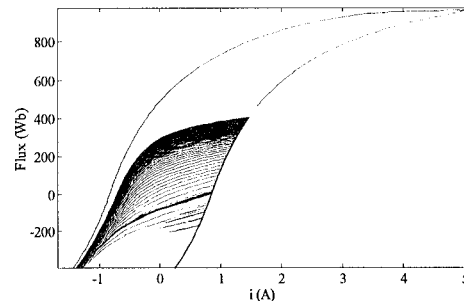

Figure 10 Hysteresis trajectories for phase-a of reenergized target transformer

It is valuable to mention that the mean number of iterations per time-point is about 2.21 and the total CPU time is 60 s for a simulation interval of 3 s using $\Delta t = 50\mu s$ on a Pentium-4 computer of 1.7 GHz. The complete network contains a total of 200 nodes and 250 devices. The simulation time is dramatically reduced by the ability of the setup to achieve steady-state conditions at simulation startup.

VI. CONCLUSIONS

This paper has presented the implementation of a new hysteretic reactor model for transient analysis. The model has been demonstrated using the EMTP-RV environment. The physical model as such, has been derived from previously

available work, but its numerical solution and implementation are new. Important problems, such as initialization, fitting and integration into a Newton solution have been presented. The model has been used in a practical test case of transformer energization. The test case solution has achieved new and not previously available simulation capabilities.

VII. REFERENCES

[1] Electromagnetic Transients Program (EMTP), EMTP-V3, Development Coordination Group of EMTP.

[2] A. Narang, E. P. Dick, R. C. Cheung "Transformer Model for ElectroMagnetic Transient Studies", CEA Report 175 T 331 G, December 1996.

[3] E. P. Dick and W. Watson, "Transformer Models for Transient Studies Based on field Measurements", IEEE Transactions on Power Apparatus and Systems, Vol. PAS-100, No. 1, January 1981, pp. 409-419.

[4] S. N. Talukdar and J. R. Bailey, "Hysteresis Model for System Studies" IEEE Transactions on Power Apparatus and Systems, Vol. PAS-95, July/August 1976, pp. 1429-1434.

[5] J. G. Frame, N. Mohan, T. Liu, "Hysteresis Modeling in an Electromagnetic Transients Program", IEEE Transactions, Vol PAS-101, No. 9, Sept. 1982, pp. 3403-3412.

[6] D. N. Ewart, "Digital Computer Simulation Model of a Steel-Core Transformer", IEEE, Transactions on Power Delivery, Vol. PWRD-1, No. 3, July 1986, pp. 174-183.

[7] H. W. Dommel, "Nonlinear and time-varying elements in digital simulation of electromagnetic transients", IEEE Transactions, Vol. PAS-90, 1971, pp. 2561-2567

[8] J. Mahseredjian, S. Lefebvre and X.-D. Do : "A new method for time-domain modeling of nonlinear circuits in large linear networks". 11th Power Systems Computation conference (PSCC), Proceedings Vol. 2, August 1993, pp. 915-922.

[9] A. Semlyen and A. Castro : "A digital transformer model for switching transient calculations in three phase systems", PICA Conference Proceedings, New Orleans, June 1975, pp. 121-126

[10] J. Mahseredjian, L. Dubé, L. Gérin-Lajoie, "New advances in the Simulation of Transients with EMTP: Computation and Visualization Techniques", Electrimacs, August 19th, 2002, Plenary session paper.

[11] J. Mahseredjian, "EMTPWorks, a graphical user interface for EMTP", Hydro-Québec, 2002